Thermodynamic Assessment of the NaCl-CrCl$_2$, NaCl-CrCl$_3$, and FeCl$_2$-CrCl$_2$ Pseudo-Binary Systems for Describing the Corrosion Chemistry Between Molten Salt Fuel and Steel

Tiwari, V.; Abbink, T. F.; Flores, J. A.Ocádiz; Flèche, J. L.; Gueneau, C.; Chatain, S.; Smith, A. L.; Martinet, J.; Venard, C.

DOI
10.1080/00295639.2023.2223745

Publication date
2023

Document Version
Final published version

Published in
Nuclear Science and Engineering

Citation (APA)
Tiwari, V., Abbink, T. F., Flores, J. A. O., Flèche, J. L., Gueneau, C., Chatain, S., Smith, A. L., Martinet, J., & Venard, C. (2023). Thermodynamic Assessment of the NaCl-CrCl$_2$, NaCl-CrCl$_3$, and FeCl$_2$-CrCl$_2$ Pseudo-Binary Systems for Describing the Corrosion Chemistry Between Molten Salt Fuel and Steel. *Nuclear Science and Engineering*, *197*(12), 3035-3057. https://doi.org/10.1080/00295639.2023.2223745

Nuclear Science and Engineering

ISSN: (Print) (Online) Journal homepage: https://www.tandfonline.com/loi/unse20

Thermodynamic Assessment of the NaCl-$CrCl_2$, NaCl-$CrCl_3$, and $FeCl_2$-$CrCl_2$ Pseudo-Binary Systems for Describing the Corrosion Chemistry Between Molten Salt Fuel and Steel

V. Tiwari, T. F. Abbink, J. A. Ocádiz Flores, J. L. Flèche, C. Gueneau, S. Chatain, A. L. Smith, J. Martinet & C. Venard

To cite this article: V. Tiwari, T. F. Abbink, J. A. Ocádiz Flores, J. L. Flèche, C. Gueneau, S. Chatain, A. L. Smith, J. Martinet & C. Venard (2023) Thermodynamic Assessment of the NaCl-$CrCl_2$, NaCl-$CrCl_3$, and $FeCl_2$-$CrCl_2$ Pseudo-Binary Systems for Describing the Corrosion Chemistry Between Molten Salt Fuel and Steel, Nuclear Science and Engineering, 197:12, 3035-3057, DOI: 10.1080/00295639.2023.2223745

To link to this article: https://doi.org/10.1080/00295639.2023.2223745

NUCLEAR SCIENCE AND ENGINEERING · VOLUME 197 · 3035–3057 · DECEMBER 2023
© 2023 The Author(s). Published with license by Taylor & Francis Group, LLC.
DOI: https://doi.org/10.1080/00295639.2023.2223745

Thermodynamic Assessment of the NaCl-$CrCl_2$, NaCl-$CrCl_3$, and $FeCl_2$-$CrCl_2$ Pseudo-Binary Systems for Describing the Corrosion Chemistry Between Molten Salt Fuel and Steel

V. Tiwari,[a,b]* T. F. Abbink,[c] J. A. Ocádiz Flores,[c] J. L. Flèche,[b] C. Gueneau,[b] S. Chatain,[b] A. L. Smith,[c]
J. Martinet,[a] and C. Venard[a]

[a]*CEA, IRESNE/DER/SPRC/LE2C, Cadarache, 13108 Saint-Paul-Lez-Durance, France*
[b]*Université Paris-Saclay, CEA, Service de la Corrosion et du Comportement des Matériaux dans leur Environnement, 91191 Gif-sur-Yvette, France*
[c]*Delft University of Technology, Faculty of Applied Sciences, Radiation Science & Technology Department, Mekelweg 15, 2629, JB Delft, The Netherlands*

Received November 21, 2022
Accepted for Publication May 23, 2023

Abstract — *A thorough understanding of the corrosion chemistry between molten salt fuel and structural materials (e.g., steel) is key for the advancement of Molten Salt Reactor technology. In this work, we consider more specifically the case of a chloride fuel salt mixture and the thermochemistry of a salt mixture such as (NaCl-$MgCl_2$-$PuCl_3$) in interaction with (Fe, Cr, Ni). The present work aims at the development of a thermodynamic model of the key subsystems NaCl-$CrCl_2$, NaCl-$CrCl_3$, and $FeCl_2$-$CrCl_2$ to predict corrosion products that may form between molten salt and structural materials. The Modified Quasichemical Model in the quadruplet approximation is used to describe the Gibbs energy of the liquid phase. A critical review of the existing phase diagram and thermodynamic data on theses systems is first presented. To alleviate the lack of data, ab initio calculations coupled with a quasi-harmonic approach are performed to estimate the thermodynamic properties for the intermediate solid compounds Na_2CrCl_4 and Na_3CrCl_6, which exist in the NaCl-$CrCl_2$ and NaCl-$CrCl_3$ systems, respectively. These atomistic simulation data together with selected experimental data are then used as input for the thermodynamic assessment of the three subsystems.*

Keywords — *Molten salt reactors, CALPHAD approach, NaCl-$CrCl_2$, NaCl-$CrCl_3$, $FeCl_2$-$CrCl_2$.*

Note — *Some figures may be in color only in the electronic version.*

I. INTRODUCTION

In Molten Salt Reactors (MSRs), the fissile material (here, $PuCl_3$) is dissolved in a molten salt mixture (NaCl-$MgCl_2$) that acts as the fuel as well as the coolant for the primary circuit. This mixture circulates in the entire reactor core and to intermediate heat exchanger units.

In the fuel, the fission products may exist in liquid or solid and/or gas states, and the elements can interact chemically with the internal structural materials. Furthermore, the molten salt in the primary circuit may be regularly circulated through a chemical treatment unit for addition of fresh fissile material and a "cleanup" of the spent fuel (i.e., removal of selected fission products from the molten salt that would otherwise act for instance as neutron poisons). Together, these processes contribute to the evolution of the molten salt fuel composition over time, which influences reactor operation.

It is thus essential to have a comprehensive knowledge of the fission product chemistry and of the corrosion products that can dissolve in the molten salt for the evaluation

---

*Email: vaishnvi.tiwari@gmail.com

of the reactor performance. In such circumstances, computational thermodynamics using the CALPHAD method[1] is a reliable tool for modeling and predicting the thermodynamic properties and phase equilibria for such complex multicomponent systems.

In this context, the present work focuses on the development of thermodynamic models using the CALPHAD method to describe the interaction between the molten salt $NaCl\text{-}MgCl_2$ and the steel components (Fe-Cr-Ni). In fact it should be noted that there exist thermodynamic models for the pseudo-binary/pseudo-ternary systems of $NaCl\text{-}MgCl_2\text{-}FeCl_2\text{-}NiCl_2$ in the works of Robelin et al.,[2,3] which reproduce well the available experimental results. However, to date, there are no models on the systems $NaCl\text{-}CrCl_2$ and $FeCl_2\text{-}CrCl_2$.

A recent work of Ard et al.[4] does describe a thermodynamic model for the system $NaCl\text{-}CrCl_3$, which is based solely on phase diagram data. There are no thermodynamic data on the liquid nor on the intermediate solid compound. In the present work, a comprehensive thermodynamic assessment of the $NaCl\text{-}CrCl_2$, $NaCl\text{-}CrCl_3$, and $FeCl_2\text{-}CrCl_2$ systems is presented, based on a critical review of all the available experimental phase diagram and thermodynamic information. To make up for the lack of thermodynamic data, the calculation of those properties for the intermediate compounds was moreover performed using density functional theory (DFT) and a quasi-harmonic model.[5] These models will be introduced in the JRCMSTDB database developed and maintained by Joint Research Centre (JRC).[6]

The paper begins with a detailed literature review on the data available on the pseudo-binary systems $NaCl\text{-}CrCl_2$, $NaCl\text{-}CrCl_3$, and $FeCl_2\text{-}CrCl_2$ and on the thermodynamic data available for the pure and intermediate compounds (in Sec. II). Following this literature review, Sec. III details the ab initio calculations for the intermediate compounds. Then, the CALPHAD approach and the thermodynamic models used for describing the different phases are presented in Sec. IV, along with the results on the new thermodynamic assessments that have been conducted (in Sec. IV.C). Finally, the conclusions are given in Sec. V.

II. LITERATURE REVIEW ON THE $NaCl\text{-}CrCl_2$, $NaCl\text{-}CrCl_3$, and $FeCl_2\text{-}CrCl_2$ SYSTEMS

II.A. Phase Diagram Data

II.A.1. $NaCl\text{-}CrCl_2$

Phase diagram investigations of the $NaCl\text{-}CrCl_2$ system have been reported by Seifert and Klatyk[7] and Shiloff.[8] Furthermore, Korshunov et al.[9] performed a review of four different phase diagram investigations for the system.

The temperature measurements by Shiloff[8] were performed using the cooling curves on an electronic potentiometer, and the concentrations of the melts were determined after cooling by standard quantitative methods. Shiloff[8] reports the presence of a single intermediate solid compound Na_3CrCl_5 that melts incongruently at $T = 731 \pm 3$ K. Additionally, the authors report the presence of a eutectic reaction: [Liquid = Na_3CrCl_5+$CrCl_2$] at $T = 710 \pm 3$ K, $x_{CrCl_2} = 0.463$. The melting point of pure $CrCl_2$ was reported as 1093 K. Figure 1 shows the experimental phase diagram given by Ref. [8].

The investigation by Seifert and Klatyk[7] was performed using differential thermal analysis. The phase diagram published in this work reports the existence of an intermediate solid compound Na_3CrCl_5 and a eutectic equilibrium. Although this study does not mention its temperature and composition values, the review work of Korshunov et al.[9] states that the most reliable experimental data points were obtained from the work of Seifert and Klatyk.[7] The latter review reports the temperature and composition values for the eutectic to be $T = 710 \pm 2$ K, $x_{CrCl_2} = 0.463 \pm 0.005$ and $T = 731 \pm 2$ K, $x_{CrCl_2} = 0.42 \pm 0.005$ for the peritectic, respectively.

By contrast with the aforementioned three works, the studies performed by Efimov et al.[10] and Shkol'nikov[11] identify different intermediate compounds. Efimov et al.[10] report the existence of solid Na_2CrCl_4 that melts incongruently through a peritectic reaction at $T = 723$ K, $x_{CrCl_2} = 0.42$ for the liquid composition. The authors also report a eutectic equilibrium at $T = 715$ K, $x_{CrCl_2} = 0.44$. Moreover, the work by Shkol'nikov[11] identifies the

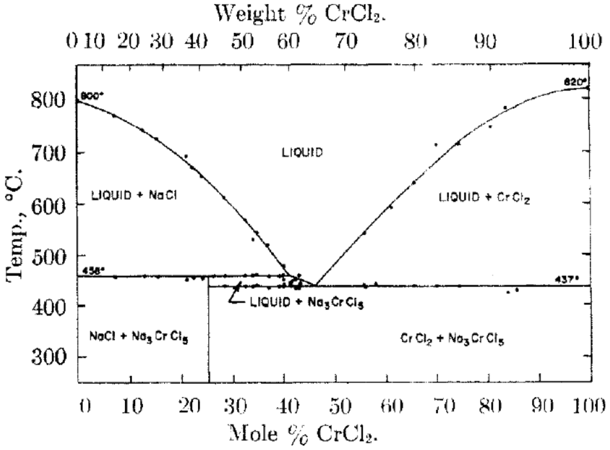

Fig. 1. Phase diagram for $NaCl\text{-}CrCl_2$ reported by Shiloff.[8] Reproduced with permission from the American Chemical Society.

TABLE I

Literature Data for the NaCl-CrCl$_2$ System*

Equilibrium Reaction	Shiloff[8]	Seifert and Klatyk[7]	Efimov et al.[10]	Shkol'nikov[11]
Eutectic $CrCl_2 + Na_xCrCl_y = L$	$T = 710 \pm 3$ K $x_{CrCl_2} = 0.463$	$T = 710 \pm 2$ K $x_{CrCl_2} = 0.463 \pm 0.005$	$T = 715$ K $x_{CrCl_2} = 0.44$	$T = 721$ K $x_{CrCl_2} = 0.460$
Peritectic $Na_2CrCl_4 = L + NaCl$			$T = 723$ K $x_{CrCl_2} = 0.42$	
Peritectic $Na_3CrCl_5 = L + NaCl$	$T = 731 \pm 3$ K $x_{CrCl_2} = 0.40$	$T = 731 \pm 2$ K $x_{CrCl_2} = 0.42 \pm 0.005$		
Peritectic $Na_4CrCl_6 = L + NaCl$				$T = 741$ K $x_{CrCl_2} = 0.39$

*For the intermediate compound Na_xCrCl_y, $x = 2, 3, 3, 4$ and $y = 4, 5, 5, 6$ for Efimov et al.,[10] Shiloff,[8] Seifert and Klatyk,[7] and Shkol'nikov,[11] respectively.

intermediate compound to be Na_4CrCl_6, which melts incongruently at $T = 741$ K, $x_{CrCl_2} = 0.39$, while the eutectic between $CrCl_2$ and Na_4CrCl_6 appears at $T = 721$ K, $x_{CrCl_2} = 0.460$. A comparison among the different studies is reported in Table I. For the present work, the data for the eutectic equilibrium [$CrCl_2$+Na_2CrCl_4= Liquid] have been selected from the works of Seifert and Klatyk[7] and Shiloff[8][a] whereas the data for the peritectic equilibrium are selected from the work of Efimov et al.[10] The choice of Na_2CrCl_4 intermediate for this system is made based on evidence from crystallography studies conducted by the Smith team at TU Delft (unpublished Master's Thesis). Recent samples of NaCl-CrCl$_2$ were prepared for differential scanning calorimetry analysis, which upon post–X-ray diffraction analysis identified the presence of Na_2CrCl_4 as the sole intermediate compound. Furthermore, Na_2CrCl_4 is the only compound that is listed in large inorganic databases such as Pearson's crystal database.[12,13]

II.A.2. NaCl-CrCl$_3$

For the NaCl-CrCl$_3$ system, four separate phase diagram investigations were carried out, out of which only three studies have been considered for the purpose of the thermodynamic assessment. The fourth study reported by Oki and Tanikawa[14] has not been taken into account as their phase diagram[14] is very different from the other three assessments. Furthermore, a thermodynamic model of the same system has been recently presented in the work of Ard et al.[4]

The first investigation was reported by Korshunov and Raskin,[15] which is based on a thermal analysis of the cooling curves. This study reports the existence of two intermediate compounds: $NaCrCl_4$ and Na_3CrCl_6. Furthermore, three invariant equilibria are reported: two eutectic points (that occur at $T = 866$ K, $x_{CrCl_3} = 0.212$ and $T = 843$ K, $x_{CrCl_3} = 0.314$, respectively) and a solid-state transition of the intermediate compound Na_3CrCl_6 at $T = 713$ K. The intermediate compound Na_3CrCl_6 is also reported to melt congruently at $T = 876$ K, $x_{CrCl_3} = 0.25$, and the melting point of pure $CrCl_3$ is taken as $T = 1423$ K.

The investigation by Cook Jr.[16] exhibits an incomplete phase diagram that was obtained by recording heating and cooling differential curves. Cook Jr. also performed X-ray diffraction analysis. This published phase diagram reports the existence of a single intermediate solid compound Na_3CrCl_6 that melts congruently at $T = 893 \pm 3$ K, $x_{CrCl_3} = 0.25$. Cook Jr.[16] also reports the solid-state transition of the intermediate compound at $T = 863 \pm 3$ K. Additional data from the phase diagram indicate two eutectic points at $T = 870 \pm 3$ K, $x_{CrCl_3} = 0.22$ and $T = 853 \pm 3$ K, $x_{CrCl_3} = 0.34$, respectively. The phase diagram shows a steep rise of the liquidus curve above the composition $x_{CrCl_3} > 0.32$.

The third study of the system reported by Vasil'kova et al.[17] is based on a differential thermographic analysis carried out between 20 and 45 mol %. The phase diagram published by Vasil'kova et al. confirms the presence of only one intermediate compound Na_3CrCl_6 that melts at $T = 883$ K and undergoes a phase transition at $T = 835$ K.

---

[a] Note that the authors considered the intermediate phase to be Na_3CrCl_5; see Table I.

The authors also confirm the existence of two eutectic points, one between NaCl-Na_3CrCl_6 at $T = 866\,K$, $x_{CrCl_3} = 0.215$ and the other between Na_3CrCl_6-$CrCl_3$ at $T = 855\,K$, $x_{CrCl_3} = 0.31$.

The fourth assessment by Oki and Tanikawa[14] is based on differential thermal analysis and room temperature X-ray diffraction. By contrast with the previous phase diagram studies, the authors report the presence of two peritectic points and one eutectic, along with the presence of two intermediate phases Na_3CrCl_6 and $NaCrCl_4$. The first peritectic reaction, $Na_3CrCl_6 = L + NaCl$, is reported to occur at $T = 848\,K$, $x_{CrCl_3} = 0.425$, whereas the second peritectic $NaCrCl_4 = L + Na_3CrCl_6$ occurs at $T = 748\,K$, $x_{CrCl_3} = 0.40$. The eutectic point is reported at $T = 723\,K$, $x_{CrCl_3} = 0.425$.

A comparison among the different studies (for the first three works) is summarized in Table II. For the assessment presented in this work, the experimental phase diagram data from the works of Korshunov and Raskin,[15] Cook Jr.,[16] and Vasil'kova et al.,[17] which are consistent, have been selected.

II.A.3. $FeCl_2$-$CrCl_2$ System

For the $FeCl_2$-$CrCl_2$ system, a single investigation was found. The phase diagram published by Soloshenko and Vil'nyanskii[18] was obtained by the differential-thermal method, where a mixture of the pure compounds was sealed and heated to 1173 K and then cooled again, to record the readings from simple as well as differential thermocouples. Soloshenko and Vil'nyanskii report the melting point for the pure end members $FeCl_2(s)$ and $CrCl_2(s)$ as $T = 943.15\,K$ and $T = 1093.15\,K$, respectively. Furthermore, the study reports no existence of an intermediate solid compound or a eutectic point. Instead, because of similar ionic radius r values ($r_{Fe^{+2}} = 0.061\,nm$ and $r_{Cr^{+2}} = 0.073\,nm$, reported from Ref. [19]), Soloshenko and Vil'nyanskii[18] state the possibility of the existence of a solid solution over the entire composition range.

II.B. Thermodynamic Data on the Compounds

Appropriate selection of the thermodynamic data for the pure compounds is a necessary condition for an accurate thermodynamic description of a system. As a result, it is imperative to compare all the available data present on the different pure compounds in question before making the choice for the thermodynamic model. A review of the existing data on the compounds NaCl, $FeCl_2$, $CrCl_2$, $CrCl_3$, and Na_3CrCl_6 is presented hereinafter.

II.B.1. NaCl

In recent studies by Van Oudenaren et al.,[20] use of the thermodynamic functions for $NaCl(s,l)$ from the IVTAN tables by Glushko et al.[21] was recommended. Van Oudenaren et al.[20] also performed an extensive study to compare the heat capacity functions for $NaCl(l)$ determined in four different studies by Dawson et al.,[22] Murgulescu et al.,[23] Plato,[24] and Pyashyenko.[25] The authors recommended selecting the average heat capacity value from the latter works for the purpose of thermodynamic modeling. The recommendations of van Oudenaren et al.[20] were followed in the present work.

II.B.2. $FeCl_2$

The thermodynamic data for $FeCl_2(s,l)$ listed in the work of Viitala et al.[26] to optimize the binary systems of $FeCl_2$-$FeCl_3$ and $FeCl_2$-$CuCl_2$ are those selected from the FactPS (pure substance) database, version 7.2. These data

TABLE II

Comparison of the Experimental Data for the NaCl-$CrCl_3$ System from the Selected Works

Equilibrium Reaction	Korshunov and Raskin[15]	Cook Jr.[16]	Vasil'kova et al.[17]
Eutectic $CrCl_3 + Na_3CrCl_6 = L$	$T = 843$ K $x_{CrCl_3} = 0.314$	$T = 853 \pm 3$ K $x_{CrCl_3} = 0.34$	$T = 855$ K $x_{CrCl_3} = 0.31$
Congruent melting $Na_3CrCl_6 = L$	$T = 876$ K $x_{CrCl_3} = 0.25$	$T = 893 \pm 3$ K $x_{CrCl_3} = 0.25$	$T = 883$ K $x_{CrCl_3} = 0.25$
Eutectic $NaCl + Na_3CrCl_6 = L$	$T = 866$ K $x_{CrCl_3} = 0.212$	$T = 870 \pm 3$ K $x_{CrCl_3} = 0.22$	$T = 866$ K $x_{CrCl_3} = 0.215$
Phase transition $Na_3CrCl_6(\alpha) = Na_3CrCl_6(\beta)$	$T = 713$ K —	$T = 863 \pm 3$ K —	$T = 835$ K —

are in close agreement with the data mentioned in the JANAF thermochemical tables.[27] In the present work, the data listed by Viitala et al.[26] were used for the purpose of thermodynamic modeling. These data are reported in Table XII.

II.B.3. CrCl$_2$

For $CrCl_2(s,l)$, a comprehensive review of the multiple data sources available in literature was performed to select $\Delta_f H_m^0(298\,K)$, $S_m^0(298\,K)$, and the C_p functions.

The standard enthalpy of formation of $CrCl_2(s)$ was derived in various studies: EMF measurements by Gee and Shelton[28]; heat capacity measurements by Stout and Chisholm[29]; solution calorimetry experiments by Gregory and Burton[30]; vapor equilibrium studies by Doerner,[31] Schukarev et al.,[32] and Jellinek and Koop[33]; critical reviews by Wagman[34] and Evans et al.[35]; data present in the SGPS Database[36]; and the IVTAN tables listed by Iorish et al.[37]

The data proposed in the IVTAN tables by Iorish et al.[37] are based on the average of the two works by Doerner[31] and Schukarev et al.[32] on vapor equilibrium data of $CrCl_2(cr) + H_2 = Cr(cr) + 2HCl$. The study by Stout and Chisholm[29] included results based on heat capacity measurements (for the temperature range of 11 to 300 K) combined with equilibrium data on $CrCl_2(cr) + H_2(g) = Cr(cr) + 2HCl(g)$ from the work of Doerner[38] and Sano.[39,40] Furthermore, a recent study on $CrCl_3$ by Mannei et al.[41] makes use of the values reported in the later edition of the National Bureau of Standards tables by Wagman[42] and the review by Barin et al.[43]

Based on this comparison, the standard enthalpy of formation value (-396.0 ± 1.7 kJ·mol^{-1}) for $CrCl_2(s)$ was selected herein by taking an average of the experimental measurements of Doerner,[31] Gregory and Burton,[30] Gee and Shelton,[28] and Stout and Chisholm.[29] The experimental data and the final selected values are given in Table III.

A similar comparison for the standard entropy $S_m^0(298\,K)$ is made herein for $CrCl_2(s)$. The data for the solid phase were obtained by comparing the SGPS data[36] to the data obtained from calorimetry measurements by Stout and Chisholm,[29] adiabatic heat capacity measurements by Anderson,[44] and the IVTAN tables by Iorish et al.[37] These values have a high correspondence to each other. The value derived by Stout and Chisholm[29] from the integration of isothermal calorimetric heat capacity measurements in the temperature range 11 to 300 K is considered the most accurate as it also takes into account the

TABLE III

Comparison of the Literature Data Available for the Standard Enthalpy of Formation Value for $CrCl_2(s)$

$\Delta_f H_m^0(298\,K)$ (kJ·mol^{-1})	Method	References
−396.72 ± 3[a]	EMF measurements	Gee and Shelton[28]
−395.47 ± 1.67[a]	Heat capacity measurements	Stout and Chisholm[29]
−398 ± 8.5[a]	Solution calorimetry	Gregory and Burton[30]
−394 ± 3[a]	Third law treatment of vapor equilibrium data	Doerner[31]
−383 ± 4	Third law treatment of vapor equilibrium data	Schukarev et al.[32]
−378 ± 8	Third law treatment of vapor equilibrium data	Schukarev et al.[32]
−399 ± 9	Third law treatment of vapor equilibrium data	Jellinek and Koop[33]
−395.4 ± 1.5	Critical review	Wagman[34]
−405.8 ± 14.6	Based on critical review	Evans et al.[35]
−395.4	Selection of experimental data	SGPS[36]
−390 ± 5	Critical review	IVTAN tables by Iorish et al.[37]
−396.0 ± 1.7		This work

[a] The data selected to calculate an average.

TABLE IV

Comparison of the Literature Data Available for the Standard Entropy Value of $CrCl_2(s)$

$S_m^0(298\,K)$ ($J \cdot K^{-1} \cdot mol^{-1}$)	Method	Temperature Range (K)	Reference
115.31 ± 0.21	Isothermal calorimetry	11 to 300	Stout and Chisholm[29]
115.3 ± 0.4[a]	Critical review[29]	—	Evans et al.[35]
115.3	Selection of experimental data	—	SGPS[36]
115.30 ± 0.3	Critical review	—	IVTAN tables by Iorish et al.[37]
114.6 ± 2.9	Adiabatic calorimetry	44 to 296	Anderson[44]

[a]The value selected in this work.

magnetic phase transition of $CrCl_2$ at 16.08 ± 0.02 K. This value (115.3 $J \cdot K^{-1} \cdot mol^{-1}$) has been selected for the present work. Iorish et al.[37] also select the value found by Stout and Chisholm[29] and state that the result is in satisfactory agreement with the results of Anderson[44] (obtained from adiabatic calorimetry measurements in the temperature range of 44 to 296 K). Furthermore, the value proposed by Evans et al.[35] was also taken from the work of Stout and Chisholm.[29] The comparison of the data and the selected value is listed in Table IV.

For the heat capacity function of $CrCl_2(s)$, the functions of Stout and Chisholm,[29] Iorish et al.,[37] and the SGPS database[36] were compared. The function for $CrCl_2(s)$ by Stout and Chisholm[29] was obtained by extrapolating the heat capacity measurements from 11 to 300 K. On the other hand, Iorish et al.[37] derived the C_p function (for the temperature range 298 to 1097 K) based on three heat capacity values: the measurement of C_p from Ref. [29] of 298.15 K and two estimated values from the experimental data by Moore[45] on the heat capacity of $MnCl_2$: C_p of 500 K and C_p of 1097 K. From these data points, the equation derived by Iorish et al. in the temperature range 298 to 1097 K [37] is given as

$$C_p(T)\left[J{\cdot}K^{-1}mol^{-1}\right] = 74.654 + 0.018236T - 7.930 \times 10^5 T^{-2} \quad . \qquad (1)$$

Two sources were considered for the enthalpy of fusion and the melting point of $CrCl_2(s)$. The first source is the SGPS database[36] that reports a value of 45 $kJ \cdot mol^{-1}$ based on a selection of experimental data. The IVTAN tables by Iorish et al.[37] report the melting temperature of $CrCl_2(s)$ as 1097 K and suggest the value of enthalpy of melting as 44 ±5 $kJ \cdot mol^{-1}$, which was estimated by taking the entropy of melting of $CrCl_2$ to be equal to the experimental entropy of melting of $MnCl_2$ (40.6 $J \cdot K^{-1} \cdot mol^{-1}$).[45] For the present work, the data proposed by Iorish et al.[37] are selected.

For the C_p function of $CrCl_2(l)$, Iorish et al.[37] propose an estimated value based on the empirical rule $C_p \approx 33n$ $J \cdot K^{-1} \cdot mol^{-1}$. Upon comparing the C_p functions for the temperature range 298.15 to 1097 K from Stout and Chisholm,[29] Iorish et al.,[37] and the SGPS database,[36] it is observed that the result from Stout and Chisholm[29] deviates the most. As a result, the present work selects the function given in the IVTAN tables from Iorish et al.[37] for $CrCl_2(s)$ and the value suggested by Iorish et al.[37] and the SGPS database[36] for $CrCl_2(l)$. The comparison between the C_p functions is given in Table V, and the final selected data are mentioned in Table XII.

II.B.4. $CrCl_3$

For $CrCl_3(s,l)$, the values for the standard enthalpy of formation $\Delta_f H_m^0(298\,K)$, entropy $S_m^0(298\,K)$, and the heat capacity function were obtained in a similar way.

The standard enthalpy of formation of $CrCl_3(s)$ was selected by comparing the data from the vapor pressure measurements by Doerner,[38] Jellinek and Koop,[33] and Matsuzaki et al.[46]; EMF measurements by Gee and Shelton[28]; solution calorimetry measurements by Schukarev et al.[47]; combustion calorimetry data by Timofeyev and Yuldasheva,[48] the SGPS database,[36] and the IVTAN tables by Iorish et al.[37] While Gee and Shelton[28] report three literature values to compare with their result from EMF measurements, the value reported in the work of Doerner[38] was calculated by studying vapor equilibria over the condensed phase mixture $CrCl_2 + CrCl_3$ and then applying the second-law method. However, the

TABLE V

Comparison of the Literature Data Available for the Heat Capacity Functions for CrCl$_2$ for Different Ranges of Temperature

Phase	C_p, T(J · K^{-1} · mol^{-1})	Temperature Range (K)	Reference
CrCl$_2(s)$	$71.96 + 0.01632\ T - 5.02 \times 10^5 T^{-2}$	300 to 1000	Stout and Chisholm[29]
CrCl$_2(s)$	$74.65 + 0.01824\ T - 7.930 \times 10^5 T^{-2} - 9.503 \times 10^{-10} T^2$	298.15 to 1097	SGPS[36]
CrCl$_2(s)$	$74.654 + 0.018236\ T - 7.930 \times 10^5 T^{-2}$ ^{a}	298.15 to 1097	IVTAN tables by Iorish et al.[37]
CrCl$_2(l)$	100^a	1097 to 3000	SGPS,[36] IVTAN tables by Iorish et al.[37]

^{a}The functions selected in this work.

measurements of Schukarev et al.[47] suggested that the latter value was too high, and thus, the authors proposed a different value by performing enthalpy of solution measurements of various metal chlorochromates and of chromium(IV) oxide in hydrogen peroxide. The value recommended in the IVTAN tables by Iorish et al.[37] is based on the result of direct calorimetric measurements by Timofeyev and Yuldasheva.[48] Furthermore, Iorish et al.[37] reject the values reported by Gee and Shelton,[28] Jellinek and Koop,[33] Matsuzaki et al.,[46] and Schukarev et al.[47] by arguing that errors arise from the choice of inaccurate thermodynamic functions, thus making the results unclear. For the present work, the values reported in the IVTAN tables by Iorish et al. are selected. The comparison of the different data and the selected value is given in Table VI.

Similar values for the standard entropy $S_m^0(298\,\mathrm{K})$ of CrCl$_3(s)$ have been reported in several sources. In their work, Hansen and Griffel[49] reported the value of 122.9 J · K^{-1} · mol^{-1} obtained from adiabatic calorimetric measurements between 15 to 300 K, taking into account the Néel point (for

TABLE VI

Comparison of the Literature Data Available for the Standard Enthalpy of Formation Value for CrCl$_3(s)$

$\Delta_f H_m^0(298\,\mathrm{K})$ (kJ·mol^{-1})	Method	References
−553 ± 5	EMF measurements	Gee and Shelton[28]
−560 ± 10	Third law treatment of vapor equilibrium data	Jellinek and Koop[33]
−556.5	Critical review	Wagman et al.[34]
−551.95 ± 20	Based on critical review	Evans et al.[35]
−570	Selection of experimental data	SGPS[36]
−544.4 ± 1.4^a	Critical review	IVTAN tables by Iorish et al.[37]
−541.76	Second law treatment of vapor equilibrium data	Doerner[38]
−516 ± 11	Third law treatment of vapor equilibrium data	Matsuzaki et al.[46]
−509.7 ± 8.36	Enthalpy of solution measurements	Schukarev et al.[47]
−544.4 ± 1.4	Combustion calorimetry	Timofeyev and Yuldasheva[48]

^{a}The value selected for this work.

TABLE VII

Comparison of the Literature Data Available for the Standard Entropy Value for $CrCl_3(s)$

$S_m^0(298\,K)(J \cdot K^{-1} \cdot mol^{-1})$	Temperature Range (K)	Method	Reference
123.0 ± 0.4	—	Based on data by Hansen and Griffel[49]	Evans et al.[35]
122.9	—	Selection of experimental data	SGPS[36]
124.7 ± 0.4^a	—	Critical review	IVTAN tables by Iorish et al.[37]
122.9	15 to 300	Adiabatic calorimetry	Hansen and Griffel[49]
122.9 ± 1.8	—	Unavailable data	Zelenina et al.[50]

[a] The selected value for present work.

the antiferromagnetic-paramagnetic phase transition) at 16.8K. Zelenina et al.[50] report a value of $122.9 \pm 1.8\ J \cdot K^{-1} \cdot mol^{-1}$ that is based on published data by Titova et al., which is unfortunately unavailable. The work of Evans et al.[35] selected the value of $123.0 \pm 0.4\ J \cdot K^{-1} \cdot mol^{-1}$ whereas in the IVTAN tables, Iorish et al.[37] argued that the result from Hansen and Griffel[49] needs to be increased by 1.7 to $124.7 \pm 0.4\ J \cdot K^{-1} \cdot mol^{-1}$ when taking into account the heat capacity measurements of Kostryukova[51] and Kostryukova and Lukyanova[52] from 2 to 20 K. Based on this comparison (presented in Table VII), the value proposed by Iorish et al.[37] is used for the present work.

As for the heat capacity functions for $CrCl_3(s)$, several sources (given in the IVTAN tables by Iorish et al.,[37] the SGPS database,[36] and the works of Zelenina et al.[50] and Hansen and Griffel[49]) were compared. The data published by Zelenina et al.[50] were obtained from another source, which unfortunately is not available. The function for $CrCl_3(s)$ over the temperature range 298 to 1200 K given by Iorish et al.[37] is derived in a similar way as for $CrCl_2(s)$, i.e., by using data points for three C_p values: a measurement of $C_p\,(298.15\,K) = 91.8\ J \cdot K^{-1} \cdot mol^{-1}$ from the work of Hansen and Griffel[49] and two estimates according to available data on the heat capacity of transition metal halides of $C_p\,(500\,K) = 100 \pm 1\ J \cdot K^{-1} \cdot mol^{-1}$ and $C_p\,(1200\,K) = 120 \pm 3\ J \cdot K^{-1} \cdot mol^{-1}$. For the liquid phase, Iorish et al.[37] estimated a value of $130\ J \cdot K^{-1} \cdot mol^{-1}$ according to the empirical rule $C_p \approx 33n\ J \cdot K^{-1} \cdot mol^{-1}$.

In this work, the functions from the SGPS database and the IVTAN tables of Iorish et al. were selected for

TABLE VIII

Comparison of the Literature Data Available for the Heat Capacity Functions for $CrCl_3$ for Different Ranges of Temperature

Phase	$C_p,\ T(J \cdot K^{-1} \cdot mol^{-1})$	Temperature Range (K)	Method	Reference
$CrCl_3(s)$	$84.92 + 0.03207\,T - 2.381 \times 10^5 T^{-2} + 2.632 \times 10^{-10} T^2\ ^a$	298.15 to 1100	Review	SGPS[36]
$CrCl_3(s)$	$88.166 + 0.026754\,T - 3.860 \times 10^5 T^{-2}$	298.15 to 1200	Fitting of heat capacity data	IVTAN tables by Iorish et al.[37]
$CrCl_3(l)$	130^a	1100 to 2500 1200 to 2000	Review Estimated	SGPS[36] IVTAN tables by Iorish et al.[37]
$CrCl_3(s)$	$86.075 + 0.03162\,T - 941.92\,T^{-1}$	600 to 1200	Source not available	Published in Zelenina et al.[50]

[a] The functions selected for this work.

the solid and liquid phases, respectively. The comparison between the different C_p functions is listed in Table VIII.

For the enthalpy of fusion and the melting temperature of $CrCl_3(s)$, the SGPS database and IVTAN tables of Iorish et al. were compared with the solubility measurements by Kerridge and Sturton.[53] The IVTAN tables by Iorish et al.[37] estimated the melting temperature of $CrCl_3(s)$ at 1200 K with an enthalpy of fusion of 48 ± 5 $kJ \cdot mol^{-1}$ (calculated from the experimental value of the entropy of melting of $MnCl_2$ from. Ref. [45]). On the other hand, the experimental work of Kerridge and Sturton[53] reports the enthalpy of fusion of $CrCl_3$ as 57.0 $kJ \cdot mol^{-1}$ by measuring the solubility of $CrCl_3$ in $ZnCl_2$ up to 870 K. This value is rejected by Iorish et al. because it is considered to be inaccurate and overestimated after recalculation of the melting point of $CrCl_3$. The value reported in the SGPS database is 60 $kJ \cdot mol^{-1}$ for a melting temperature of 1100 K. Such a low melting temperature and selected value for the transition enthalpy are not compatible with the phase diagram data (see Sec. IV.C). In this work, the enthalpy of fusion was taken from the experimental work of Kerridge and Sturton[53] while the melting temperature was taken equal to 1425 K, which matches the available phase diagram equilibrium data. It is clear that the measurement of those data would be very helpful to improve the description in the future.

II.B.5. Na_3CrCl_6

There exist few data on the thermodynamic functions of Na_3CrCl_6 in the literature. The work of Schukarev et al.[47] states two values for the standard enthalpy of formation of Na_3CrCl_6. The first value of −1739.2 $kJ \cdot mol^{-1}$ was obtained by Vasil'kova et al.[54] from measured heats of dissolution of the intermediate solid and reference substance CrO_3 in alkali solution containing hydrogen peroxide. The second value of −1742.2 $kJ \cdot mol^{-1}$ (from the work of Schukarev et al.[55]) was obtained from the heats of dissolution of Na_3CrCl_6, $CrCl_3$, and NaCl measured in hydrochloric acid solution.

It should be noted that apart from the missing data on Na_3CrCl_6, there is a complete lack of thermodynamic information on the intermediate solid Na_2CrCl_4. These data can be obtained from the ab initio calculations. Section III presents a brief description of the ab initio method and reports the results obtained for the thermodynamic functions of the intermediate compounds Na_2CrCl_4 and Na_3CrCl_6.

III. AB INITIO CALCULATIONS

Since the thermodynamic functions of Na_2CrCl_4 were not found in the literature and existing data for Na_3CrCl_6 are scarce, an ab initio study was undertaken to fill in the data gap for these compounds. The method consists of a free energy calculation at the quasi-harmonic approximation (QHA) level with the assistance of ab initio calculations. The advantage of this approach is that it requires only the parameters associated with the symmetry group, the lattice parameters of the unit cell, and the atom position coordinates to perform the calculations. An ab initio calculation code for the electronic structure of solids is used. The complete method by Flèche is presented in Ref. [5]. In this paper, only the main steps of the calculations are reported.

The following three approximations are used to derive the free energy of the crystal containing N cells with n atoms per cell:

1. The adiabatic approximation to calculate the total energy of the crystal $E(V)$ versus the volume. $E(V)$ is the total energy of the static lattice in which each atom occupies its mean position.

2. The harmonic approximation to calculate the $3n$ vibrational frequencies $\nu_j(\vec{q})$ $(j = 1, 3n)$ for N values of wave vector $\vec{q}$ in the first Brillouin zone. These $3n$ frequencies' dispersion branches are divided into three acoustic branches and $(3n - 3)$ optical branches. In order to make ab initio computations tractable, these vibrational frequencies are calculated at the Γ point only $(\vec{q} = 0)$. For $\vec{q} \neq 0$, we use the Debye model to determine the acoustic vibrational frequencies and the Einstein model for the optical vibrational frequencies. From $E(V)$ and the frequencies $\nu_j(\vec{q})$ $(j = 1, 3n)$, it is then possible to construct the partition function of the crystal and deduce its free energy at temperature T from the statistical thermodynamic laws:

$$F(T,v) = E(V) + Nk_BT\left[\begin{array}{l}\frac{9}{8}x_D + 3ln\left(1 - e^{-x_D}\right) - D(x_D) \\ + \sum_{j=4}^{3n}\left(\frac{x_j}{2} + ln\left(1 - e^{x_j}\right)\right)\end{array}\right], \quad (2)$$

where $x_j = h\nu_j(0)/k_BTD(x_D)$ = Debye function with $x_D = \Theta_D/T$, with Θ_D = Debye temperature, and k_B and

h = Boltzmann and Planck constants, respectively. For an ideal isotropic crystal, Θ_D is given in Ref. [5]:

$$\Theta_D = \frac{h}{k_B}\left(\frac{9}{4\pi V}\right)^{1/3}\left(3\frac{B}{\rho}\right)^{1/2}\left(\frac{1-\sigma^0}{1+\sigma^0}\right)^{1/2}\left(1+2\left(\frac{2-2\sigma^0}{1-2\sigma^0}\right)^{3/2}\right)^{-1/3} , \tag{3}$$

where B = bulk modulus, ρ = density, and σ^0 = Poisson ratio (close to the value 0.33).

3. To account for the thermal expansion while maintaining the simplicity of the harmonic model, a QHA is used assuming that the vibrational frequencies change with the volume of the unit cell:

$$pV = -\left(\frac{dF(T,V)}{dV}\right)_T V = -V\frac{dE(V)}{dV} + Nk_BT\left[\gamma_{ac}\left(\frac{9}{8}x_D + 3D(x_D)\right) + \gamma_{op}\sum_{j=4}^{3n}\left(\frac{x_j}{2} + \frac{x_j}{e^{x_{j-1}}}\right)\right] , \tag{4}$$

where γ_{ac} and γ_{op} = acoustic and optic Gruneïsen parameters, respectively. For an ideal isotropic crystal and under several assumptions, these Gruneïsen parameters are given in Ref. [5]:

$$\gamma_{ac} = -\frac{2}{3} - \frac{1}{2}V\frac{d}{dV}ln\left(\frac{d^2E(V)}{dV^2}\right) = \frac{B'(V)}{2} - \frac{1}{6} \tag{5}$$

$$\gamma_{op} = \frac{1}{2}V\frac{d}{dV}ln\left(\frac{d^2E(V)}{dV^{2/3}}\right) = \frac{B(V)}{2}\frac{(3B'(V)-2)}{(3B(V)-2P_{static}(V))} - \frac{1}{6} , \tag{6}$$

where $B'(V)$ is the derivative of the bulk modulus with respect to pressure.

The volume V is calculated iteratively with Eq. (4) for a given pressure p (here, 1 atm) and temperature T, knowing $E(V)$ and the vibrational frequencies at the Γ point, as well as the Poisson ratio σ^0 for the crystal to zero static pressure. All the thermodynamic functions are calculated from $F(T,V)$ and pV (see the work by Flèche[5] for reference):

1. Entropy $S = -(dF/dT)_V$.
2. Internal energy $U = F + TS$.
3. Enthalpy $H = U + pV$.
4. Bulk modulus $B = -V(dp/dT)_T$.
5. Thermal expansion $\alpha_p B = (dp/dT)_V$.
6. Heat capacity at constant volume $C_V = (dU/dT)_V$.
7. Heat capacity at constant pressure $C_p = C_V + TVB\alpha_p{}^2$.

The calculations [$E(V)$ and the vibrational frequencies at the Γ point] were performed using the CASTEP code,[56] which solves the electronic Schrödinger equation for a compound with a periodic lattice within the electronic DFT using a plane-wave pseudopotential method. The exchange/correlation energy used is the Perdew et al. form [Perdew-Burke-Ernzerhof for solids (PBEsol)] of the generalized gradient approximation.[57] The first Brillouin zone is approximated with finite sampling of k-points using the Monkhorst-Pack scheme.[58] The tightly bound core electrons are represented by ultrasoft pseudopotentials (generated on the fly) as proposed by the CASTEP server code.

Furthermore, when the electron spins of the ions are unpaired, the calculations are carried out using polarized spins. Na$_2$ (Cr^{2+}, with four unpaired electrons) Cl$_4$ and Na$_3$ (Cr^{3+}, with three unpaired electrons) Cl$_6$ are considered to be ferromagnetic compounds. The results obtained after geometry optimization with the CASTEP code at zero static pressure are given in Table IX.

The formation enthalpies and standard entropies are obtained using the formation reactions of Na$_2$CrCl$_4$, Na$_3$CrCl$_6$ from the binary compounds NaCl, CrCl$_2$, and CrCl$_3$ whose thermodynamic and crystallographic data are known:

$$2\text{NaCl} + \text{CrCl}_2 = \text{Na}_2\text{CrCl}_4 \tag{7}$$

$$\begin{aligned}\Delta_f H_m^0(\mathrm{Na_2CrCl_4}) &= 2\Delta_f H_m^0(\mathrm{NaCl}) + \Delta_f H_m^0(\mathrm{CrCl_2}) + H_m^0(\mathrm{Na_2CrCl_4}) \\ &\quad -2H_m^0(\mathrm{NaCl}) - H_m^0(\mathrm{CrCl_2})\end{aligned} \tag{8}$$

$$3\mathrm{NaCl} + \mathrm{CrCl_3} = \mathrm{Na_3CrCl_6} \tag{9}$$

$$\begin{aligned}\Delta_f H_m^0(\mathrm{Na_3CrCl_6}) &= 3\Delta_f H_m^0(\mathrm{NaCl}) + \Delta_f H_m^0(\mathrm{CrCl_3}) + H_m^0(\mathrm{Na_3CrCl_6}) \\ &\quad -3H_m^0(\mathrm{NaCl}) - H_m^0(\mathrm{CrCl_3})\end{aligned}\ . \tag{10}$$

The formation entropies at 298.15K for the intermediate compounds are calculated from the standard formation reaction:

$$\Delta S_f(\mathrm{Na_2CrCl_4}) = S_m^0(\mathrm{Na_2CrCl_4}) - 2S_m^0(\mathrm{Na}) - 2S_m^0(\mathrm{Cl_2}) - S_m^0(\mathrm{Cr}) \tag{11}$$

$$\Delta S_f(\mathrm{Na_3CrCl_6}) = S_m^0(\mathrm{Na_3CrCl_6}) - 3S_m^0(\mathrm{Na}) - 3S_m^0(\mathrm{Cl_2}) - S_m^0(\mathrm{Cr}). \tag{12}$$

The values for $\Delta_f H_m^0(\mathrm{NaCl}), \Delta_f H_m^0(\mathrm{CrCl_2}), \mathrm{and} \Delta_f H_m^0(\mathrm{CrCl_3})$ are the values selected for the present work (see Sec. II); $S_m^0(\mathrm{Na}), S_m^0(\mathrm{Cl_2}), \mathrm{and} S_m^0(\mathrm{Cr})$ are tabulated at 298.15 K in Ref. [61]; $H_m^0(\mathrm{NaCl})$, $H_m^0(\mathrm{CrCl_2})$, $H_m^0(\mathrm{CrCl_3})$, $H_m^0(\mathrm{Na_2CrCl_4})$, $H_m^0(\mathrm{Na_3CrCl_6})$, $S_m^0(\mathrm{Na_2CrCl_4})$, and $S_m^0(\mathrm{Na_3CrCl_6})$ are calculated versus the temperature with the method presented here in Table X.

For the two intermediate solids, the C_p functions obtained from the ab initio approach with the QHA model were compared with those obtained by the applying the Neumann-Kopp rule to the C_p functions of the pure end members. The functions obtained from the two approaches and the C_p values at 298 K are listed in Table XI.

The C_p functions calculated with the QHA strongly depend on the bulk modulus and its derivative with the pressure. For the present systems under consideration (i.e., NaCl, CrCl$_2$, and CrCl$_3$), these parameters are very dependent on the soft character of the solids. As a result, for these compounds the C_p functions tend to diverge at low temperatures (see Figs. 2 and 3), thus limiting our confidence in the QHA model. Consequently, the functions obtained from the Neumann-Kopp approximation have been selected for the present work.

Based on these calculations and the comparison among all the data from different sources, the selected values of $\Delta_f H_m^0(298\,\mathrm{K})$, $S_m^0(298\,\mathrm{K})$, and C_p for the pure solids and liquids (i.e., the end members) as well as the intermediate solid compounds are listed in Table XII. These data were used in the thermodynamic assessment of the systems in Sec. IV.C.

IV. THERMODYNAMIC MODELING USING THE CALPHAD METHOD

The Gibbs energy of a phase θ is described in the CALPHAD model with the following general expression:

$$G_M^\theta = G_M^{(\theta srf)} + G_M^{(\theta cfg)} + G_M^{(\theta E)}\quad , \tag{13}$$

where

$G_M^{(\theta srf)}$ = reference Gibbs energy, equal to the sum of the Gibbs energy of the pure end members

$G_M^{(\theta cfg)}$ = contribution from the assumption of an ideal mixing of the species, corresponding to all the possible configurations in which they can exist

$G_M^{(\theta E)}$ = excess Gibbs energy.

The model parameters representing the excess Gibbs energy contribution are fitted based on the available experimental data obtained from phase diagram investigations, enthalpy of mixing, calorimetry, solubility limit studies, etc., and/or results of ab initio calculations in order to best reproduce the thermodynamic properties of the system.

For the present work, the solid solutions have been modeled using the Substitutional Regular Solution Model whereas the liquid phases have been modeled using the Modified Quasi-chemical Model in Quadruplet Approximation (MQMQA).

IV.A. Substitutional Regular Solution Model to Describe Solid Phases

In this model, the species (A, B) are assumed to randomly mix on a single sublattice.[62] The contribution

TABLE IX

Ab Initio Calculations of the Na$_2$CrCl$_4$ and Na$_3$CrCl$_6$ Parameters Using the CASTEP Code[56] Compared to the Reference Experimental Data from Pearson's Crystal Data[59]*

		Z	a (Å)	b (Å)	c (Å)	α	β	γ	V_0(Å)^3	B_0 (GPa)	B_0'	Total Magnetization, μB/Cr	Band Gap (eV)
Na$_2$CrCl$_4$	Experiment	2	3.9407	11.5905	6.9618	90	92.465	90	317.684				
	Calculation	2	3.9368	11.3351	6.9122	90	92.467	90	308.160	25.1	5.66	4.12	0.636
Na$_3$CrCl$_6$	Experiment	2	6.82	6.82	12.034	90	90	120	484.741				
	Calculation	2	6.807	6.807	11.899	90	90	120	477.582	20.5	5.08	3.19	1.76

*Bulk modulus and its derivative with respect to pressure at zero pressure are obtained with a fit of the Vinet equation of state.[60]

terms $G_M^{(\theta srf)}$ and $G_M^{(\theta cfg)}$ for the Gibbs energy of the phase are expressed as

$$G_M^{(\theta srf)} = X_A G_A{}^{\theta}(T) + X_B G_B{}^{\theta}(T) \tag{14}$$

$$G_M^{(\theta cfg)} = RT(X_A lnX_A + X_B lnX_B) \quad , \tag{15}$$

where X_i = site fraction in the sublattice (in this case, X_i is equal to the mole fraction x_i of the component for i = A, B) and G_i^{θ} = molar Gibbs free energy of the end member. It should be noted that in the present work, the term for the end members refers to the individual base salts. The third contributing term $G_M^{(\theta E)}$ can be expressed as a simple polynomial of the following form:

$$G_M^{(\theta E)} = \Sigma q_{AB}^{ij} X_A^i X_B^j \quad , \tag{16}$$

where the interaction parameter q_{AB}^{ij} may depend on temperature T.

IV.B. Modified Quasi-Chemical Model for the Molten Salt

The ionic liquids (molten salts) tend to exhibit large deviations from ideal mixing due to the presence of very strong short range ordering (SRO) at the first nearest neighbors (FNNs) and second nearest neighbors (SNNs), i.e., interactions between cation-anion (FNNs) and cation-cation (or anion-anion) (SNN) pairs, respectively. These structural interactions have a significant impact on the energetics of the system, which also depend on changing temperature and composition.

MQMQA is used to describe this phase[63,64] as it allows one to select the composition of maximum SRO by specifying the ratio between the cation-cation coordination numbers Z_{AB}^A and Z_{AB}^B. In MQMQA, the molten system is composed of ionic liquids with the same (or different) anion and different cations (e.g., A-X, B-Y, where A, B represent cations and X, Y represent anions). Within the context of the present work, binary systems with a common anion (i.e., $X = \mathrm{Cl}^-$) are considered. The MQMQA model, developed in Refs. [65] through [68], assumes that the cations A,B and the anion X are distributed on two sublattices. The FNN and SNN pairs (of the types A-X-A, B-X-B, and A-X-B) can then be represented as quadruplets, which becomes the basic unit for the model. The pair exchange reaction between the SNNs is expressed by Fig. 4.

TABLE X

Entropy and Enthalpy of Formation Calculated for Na_2CrCl_4 and Na_3CrCl_6

1 atm	Group	$\Delta_f H_m^0$ (kJ·mol^{-1}) 298.15 K	S_m^0 (JK^{-1}mol^{-1}) 298.15 K	C_p (JK^{-1}mol^{-1}) 298.15 K	H_m^0 This Work (DFT) (kJ·mol^{-1}) 298.15 K	S_m^0 This Work (DFT) (JK^{-1}mol^{-1}) 298.15 K	C_p This Work (DFT) (JK^{-1}mol^{-1}) 298.15 K	$\Delta_f H_m^0$ This Work (DFT) (kJ·mol^{-1}) 298.15 K	ΔS_m^0 This Work (DFT) (JK^{-1}mol^{-1}) 298.15 K
Na			51.21						
Cr			23.54						
Cl_2			222.96						
NaCl	F4/M-32/M 225	−411.26	72.15	50.49	−167 315.84	74.76	53.12		
$CrCl_2$	P21/N21/ N2/M 58	−396	115.3	71.17	−318 933.69	106.84	74.11		
$CrCl_3$	R-3 148	−544.4	124.7	91.80	−360 477.89	126.33	97.10		
Na_2CrCl_4	P121/C1 14				−653 560	259.16	185.06	−1218.51	−312.72
Na_3CrCl_6	P-312/C 163				−862 418.51	354.52	258.14	−1778.17	−491.53

The term $\Delta g_{(AB/X)}$ denotes the excess Gibbs energy associated with the pair exchange reaction. Physically, it depicts whether the formation of A-B-X quadruplet pairs is favorable [when $\Delta g_{(AB/X)} < 0$] or not. In the MQMQA model, the term $\Delta g_{(AB/X)}$ is an adjustable model parameter, which can be expressed in the form of a simple polynomial[69] expressed as

$$\Delta g_{AB/X} = \Delta g^0{}_{AB/X} + \Sigma_{i\geq 1} g^{i0}{}_{AB/X}\chi^i_{AB/X} + \Sigma_{j\geq 1} g^{0j}{}_{AB/X}\chi^j_{BA/X} \quad , \tag{17}$$

where the terms $\Delta g^0{}_{AB/X}$ and $g^{ij}{}_{AB/X}$ are composition independent coefficients that may depend on temperature. To take into account the composition dependence, the term $\chi_{AB/X}$ is introduced, which is defined in terms of the cation-cation pair fractions X_{ij} as

$$\chi_{AB/X} = \frac{X_{AA}}{(X_{AA} + X_{BB} + X_{AB})} \quad . \tag{18}$$

TABLE XI

C_p Functions Obtained for the Intermediate Compounds Na_2CrCl_4 and Na_3CrCl_6 : Comparison Between the Ab Initio Approach and the Neumann-Kopp Approximation

Compound	$C_p(T)_{ab-initio}$ (JK^{-1}mol^{-1})	$C_p(298\,\mathrm{K})_{ab-initio}$ (JK^{-1}mol^{-1})	$C_p(T)_{N.K.}$^{a}(JK^{-1}mol^{-1})	$C_p(298\,\mathrm{K})_{N.K.}$^{a} (JK^{-1}mol^{-1})
Na_2CrCl_4	$167.6704 + 0.0896\,T$ $-1.3582 \times 10^{-5}T^2$ $-\ 720858.48\ T^{-2}$	185.06	$170.0972 + 0.0296\,T$ $+2.4293 \times 10^{-5}T^2$ $-\ 794\ 765.992\ T^{-2}$	172.14
Na_3CrCl_6	$241.0484 + 0.1070\,T$ $-1.2604 \times 10^{-5}T^2$ $-\ 1219397.9\ T^{-2}$	258.14	$228.08474 + 0.04917\,T$ $+3.64400632 \times 10^{-5}T^2$ $-\ 240\ 748.9\ T^{-2}$	243.27

[a] N.K. = Neumann-Kopp.

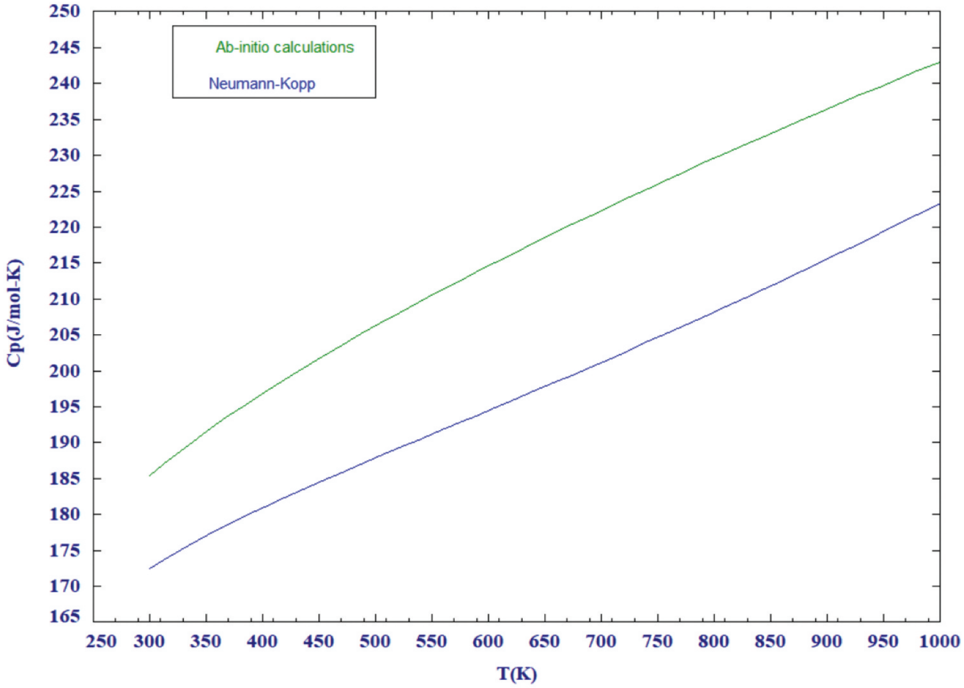

Fig. 2. Comparison of the C_p functions obtained from the ab initio calculations and the Neumann-Kopp rule for the intermediate solid Na_2CrCl_4.

It should be noted that in cases where liquids exhibit very strong SRO, it is recommended to define the cation-cation coordination numbers (denoted as Z^A_{AA}, Z^B_{BB} and Z^A_{AB}, Z^B_{AB}) that are dependent on the composition of the liquid.[70] These factors are not explicitly required in the configurational entropy terms, but they must be accurately determined for each quadruplet in order to have accurate representation of the molten salt SRO

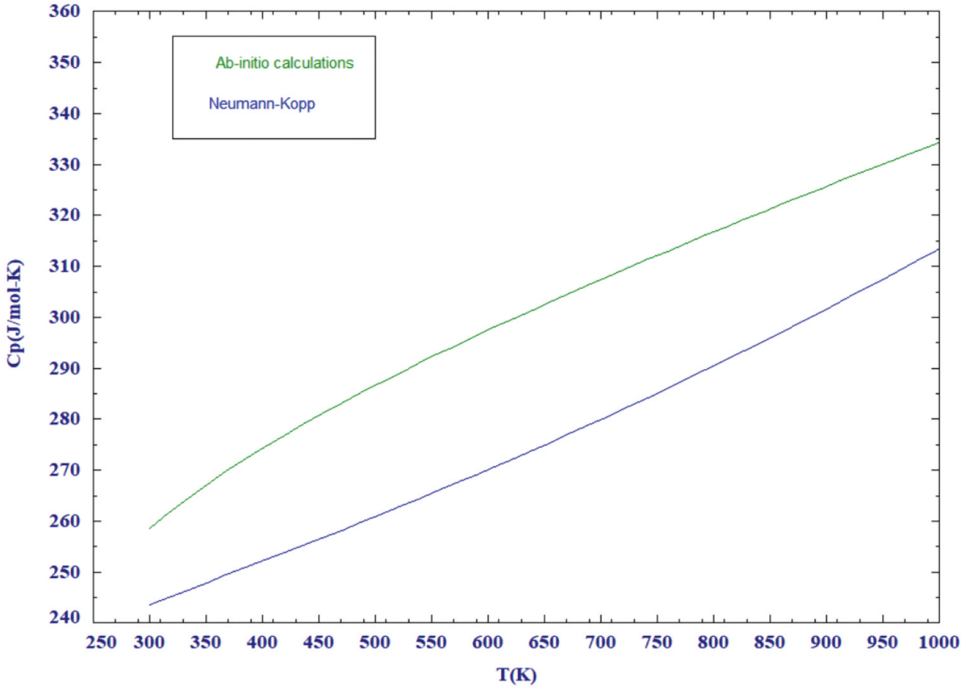

Fig. 3. Comparison of the C_p functions obtained from the ab initio calculations and the Neumann-Kopp rule for the intermediate solid Na_3CrCl_6.

TABLE XII

Selected Thermodynamic Data for Compounds*

Compound	Temperature Range (K^1)	$\Delta_f H_m^0(298\,K)$ $(kJ{\cdot}mol^{-1})$	$S_m^0(298\,K)$ $(JK^{-1}mol^{-1})$	$C_p(T)$ $(JK^{-1}mol^{-1})$	Reference
$NaCl(s)$	298 to 1074	−411.26	72.15	$47.7216 + 0.0057\,T - 882.996\,T^{-2} + 1.2147 \times 10^{-5}T^2$	IVTAN tables by Glushko et al.[21]
$NaCl(l)$	298 to 2000	−390.85	83.30	68.0	Van Oudenaren et al.[20]
$CrCl_2(s)$	298 to 1097	−396	115.3	$74.654 + 0.0182\,T - 7.930 \times 10^5 T^{-2}$	Stout and Chrisholm,[29] Evans et al.[35]
$CrCl_2(l)$	298 to 3000	−364.02	132.8	100	SGPS,[36] IVTAN tables by Iorish et al.[37]
$CrCl_3(s)$	298 to 1425	−544.4	124.7	$84.92 + 0.03207\,T - 238\,100\,T^{-2} + 2.632 \times 10^{-10}T^2$	SGPS,[36] IVTAN tables by Iorish et al.[37]
$CrCl_3(l)$	298 to 2500	−507.694	129.0	130	SGPS,[36] IVTAN tables by Iorish et al.[37]
$FeCl_2(s)$	298 to 950	−341.83	117.95	$82.8034 + 6.8044 \times 10^{-3}\,T - 107\,285\,T^{-2} - 2075.2\,T^{-1}$	Viitala et al.[26]
$FeCl_2(l)$	298 to 2000	−311.33	139.89	102.173	Viitala et al.[26]
$Na_2CrCl_4(s)$	298 to 1074	*−1222.9(05)*	*261.59*	$170.0972 + 0.0296\,T + 2.4293 \times 10^{-5}T^2 - 794\,765.992\,T^{-2}$	This work
$\alpha - Na_3CrCl_6(s)$	298 to 1425	*−1794.2*	*351.02*	$228.0847 + 0.0492\,T + 3.6440 \times 10^{-5}T^2 - 240\,748.9\,T^{-2}$	This work
$\beta - Na_3CrCl_6(s)$	298 to 1425	*−1786.2*	*360.29*	$228.0847 + 0.0492\,T + 3.6440 \times 10^{-5}T^2 - 240\,748.9\,T^{-2}$	This work

*The values optimized during system modeling are in italics.

across the composition range. However, for the present systems, constant values have been used for the cation-cation coordination numbers, which are presented in Sec. IV.C.

IV.C. Results of the Thermodynamic Assessments

This section describes the thermodynamic models developed for the pseudo-binary systems $NaCl-CrCl_2$,

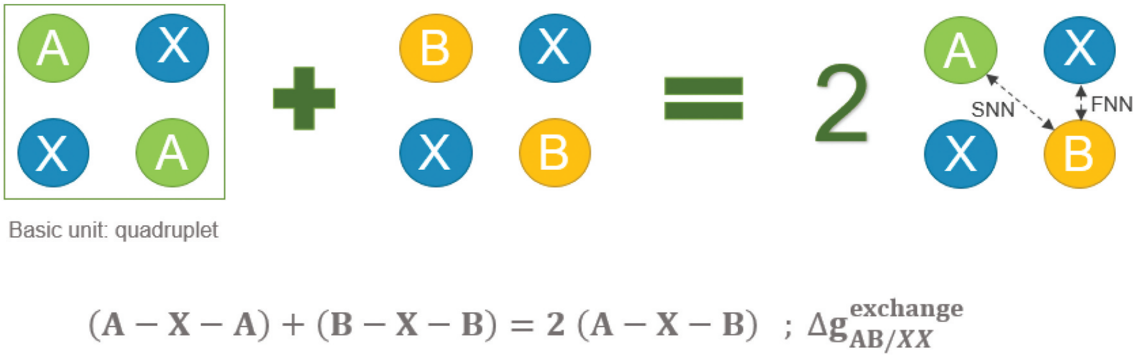

Fig. 4. Pair exchange reaction between the SNN pairs in common anion systems.

NaCl-CrCl$_3$, and FeCl$_2$-CrCl$_2$ and discusses the comparison between the calculated and available literature data.

IV.C.1. NaCl-CrCl$_2$ System

For the NaCl-CrCl$_2$ system, the SNN coordination numbers were set to the following values:

$$Z^{\mathrm{Na}}_{\mathrm{NaCr(II)}} = Z^{\mathrm{Cr(II)}}_{\mathrm{NaCr(II)}} = 6 \tag{19}$$

$$Z^{\mathrm{Cl}}_{\mathrm{NaCr(II)}} = 4\ . \tag{20}$$

The latter value of the coordination number was selected to reflect the eutectic composition in the phase diagram, where the maximum SRO is expected (composition of lowest Gibbs energy of mixing).[b] The excess Gibbs energy $\Delta g_{\mathrm{NaCr(II)/Cl}}$ $[\mathrm{J\cdot mol^{-1}}]$ associated with the quadruplet exchange reaction was optimized and expressed as

$$\begin{aligned}\Delta g_{\mathrm{NaCr(II)/Cl}} = &-(7390+3.71T)\\ &-(2900-2.5T)\chi_{\mathrm{NaCr(II)/Cl}}\\ &-(3050-2.75T)\chi_{\mathrm{Cr(II)Na/Cl}}\ .\end{aligned} \tag{21}$$

In addition to the optimization of $\Delta g_{\mathrm{NaCr(II)/Cl}}$, the thermodynamic functions associated with the enthalpy of formation $\Delta_f H^0_m(298\,\mathrm{K})$, entropy $S^0_m(298\,\mathrm{K})$, and specific heat capacity C_p functions for the intermediate solid are required for a complete assessment. As mentioned in Sec. II, the present work recognizes Na$_2$CrCl$_4$ as the sole intermediate compound. For the thermodynamic model, the thermodynamic functions for the enthalpy of formation and the entropy were optimized[c] on the basis of the data selected in Sec. II whereas the C_p functions were calculated with the help of the additive Neumann-Kopp rule. These functions and their comparison with the values obtained from the ab initio calculations are reported in Table XIII. The thermodynamic functions (except the C_p function; see the discussion in Sec. III) initially obtained from the ab initio calculations are in good agreement (with differences of 0.36% and 0.94% for enthalpy of formation and entropy, respectively) with the optimized values that have been used for the present assessment.

The calculated phase diagram for the system is depicted in Fig. 5.

A comparison between the calculated and the experimental data for the invariant reactions is reported in Table XIV. A major difference is with respect to the choice of the composition of the intermediate solid compound. The works of Seifert and Klatyk[7] and Shiloff[8] report Na$_3$CrCl$_5$ as an intermediate compound whereas for the present work, Na$_2$CrCl$_4$ has been considered. Nonetheless, there is still good agreement between the experimental and the calculated eutectic points, with a difference of approximately 3% for composition and less than 0.2% for temperature. The calculated melting temperature of 735 K found for the intermediate compound Na$_2$CrCl$_4$ is also in good agreement with the melting temperatures found for Na$_3$CrCl$_5$ of 731 ± 2 K and 731 ± 3 K in the work of Seifert and Klatyk[7] and Shiloff,[8] respectively.

---

[b] To the authors' knowledge, no structural studies of the NaCl-CrCl$_2$ system have been reported in the literature.

[c] The determination of the uncertainties on both the optimized thermodynamic parameters and the thermodynamic and phase diagram calculated data requires the use of a Bayesian approach, as recently applied for the modeling of the U-Te system by Gueneau et al.[71] This is an important subject that is not yet addressed much within the Calphad community. This kind of analysis of interest for the molten salt systems will be used in the future; hence, at this stage, no uncertainties have been assigned to the values of the assessed thermodynamic parameters $\Delta_f H^0_m(298\,\mathrm{K})$, entropy $S^0_m(298\,\mathrm{K})$ in Table XIII.

TABLE XIII

Optimized Thermodynamic Functions for the Intermediate Compound Na_2CrCl_4 Used for the Present Work and Their Comparison with the Values Obtained from the Ab Initio Calculations

Thermodynamic Functions	$\Delta_f H^0{}_m$(298 K) (kJ·mol^{-1})	S^0_m(298 K) (JK^{-1}mol^{-1})	$C_p(T)$ (JK^{-1}mol^{-1})	C_p(298 K) (JK^{-1}mol^{-1})
Optimized functions	−1222.90	261.59	$170.0972 + 0.0296\ T + 2.4293 \times 10^{-5} T^2 - 794\,765.992\ T^{-2}$	172.14
Ab initio calculations	−1218.51	259.16	$167.6704 + 0.0896\ T - 1.3582 \times 10^{-5} T^2 - 720\,858.48\ T^{-2}$	185.06

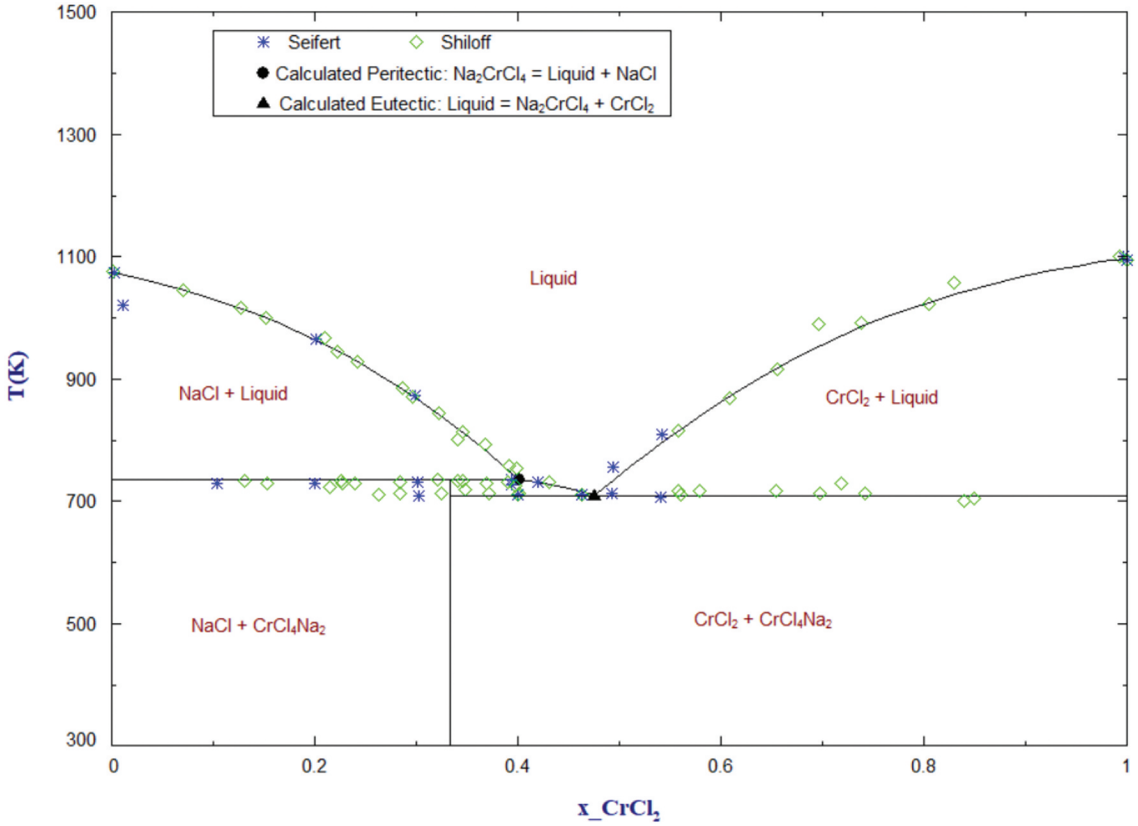

Fig. 5. Calculated phase diagram x_{CrCl_2} versus T[K] for NaCl-CrCl$_2$ system. Comparison with the experimental phase diagram data of Seifert and Klatyk[7] and Shiloff.[8]

TABLE XIV

Comparison Between the Experimental and the Calculated Eutectic and Peritectic Points for the NaCl-CrCl$_2$ System

Equilibrium Reaction	Calculated Value	Shiloff[8]	Seifert and Klatyk[7]
Eutectic $CrCl_2 + Na_xCrCl_y = L$	$x_{CrCl_2} = 0.4759$ $T = 709$ K	$x_{CrCl_2} = 0.463$ $T = 710 \pm 3$ K	$x_{CrCl_2} = 0.463 \pm 0.005$ $T = 710 \pm 2$ K
Peritectic $Na_2CrCl_4 = L + NaCl$	$x_{CrCl_2} = 0.4007$ $T = 735$ K		
Peritectic $Na_3CrCl_5 = L + NaCl$		$x_{CrCl_2} = 0.40 T = 731 \pm 3$ K	$x_{CrCl_2} = 0.42 \pm 0.005$ $T = 731 \pm 2$ K

TABLE XV

Optimized Thermodynamic Functions for the Intermediate Compound Na_3CrCl_6 Used for the Present Work and Their Comparison with the Values Obtained from Literature Review and Ab Initio Calculations

Thermodynamic Functions	$\Delta_f H^0{}_m$(298 K) (kJ·mol^{-1})	S^0_m(298 K) (JK^{-1}mol^{-1})	$C_p(T)$ (JK^{-1}mol^{-1})	C_p(298 K) (JK^{-1}mol^{-1})
Optimized functions	−1794.2	351.02	$228.08474 + 0.04917\ T + 3.64400632 \times 10^{-5} T^2 - 240\ 748.9\ T^{-2}$	243.27
Ab initio calculations	−1778.17	354.52	$241.0484 + 0.1070\ T - 1.2604 \times 10^{-5} T^2 - 1\ 219\ 397.9\ T^{-2}$	258.14
Schukarev et al.[47]	−1739.2			

IV.C.2. NaCl-CrCl$_3$ System

The SNN coordination numbers in the NaCl-CrCl$_3$ system were set to the following values, again selected to match the expected composition of maximum SRO[d]:

$$Z^{Na}_{NaCr(III)} = 3 \tag{22}$$

$$Z^{Cr(III)}_{NaCr(III)} = 6 \tag{23}$$

$$Z^{Cl}_{NaCr(III)} = 2.4\ . \tag{24}$$

The excess Gibbs energy associated with the quadruplet exchange reaction $\Delta g_{NaCr(III)/Cl}$ $[\mathrm{J \cdot mol^{-1}}]$ was optimized and expressed as

$$\begin{aligned}\Delta g_{NaCr(III)/Cl} &= (-17000) - (1400 + 1.55T)\chi_{NaCr(III)/Cl} \\ &+ (2000)\chi_{Cr(III)Na/Cl}\end{aligned}\ . \tag{25}$$

In the present work, the thermodynamic functions associated with the enthalpy of formation $\Delta_f H^0_m(298)$ and entropy $S^0_m(298)$ for the intermediate solid Na_3CrCl_6 obtained from the ab initio calculations were further optimized. For the heat capacity C_p function of the intermediate solid, the additive Neumann-Kopp rule was applied. The optimized functions and C_p functions used in the present work, along with their comparison with the ab initio calculations and the data obtained from literature review, are reported in Table XV. These data obtained from the ab initio approach (except the C_p functions; see Sec. III) are in good agreement (with a difference of 0.90% and 0.98% for enthalpy of formation and entropy, respectively) with the optimized value used for the present assessment as well as the value reported in the work of Schukarev et al.[47] (relative error percent 3.16%).

Additionally, the solid-state transition for Na_3CrCl_6 was also taken into account. This was achieved by defining a second solid phase, and an enthalpy value associated with this transition was set to

$$\Delta H_{transition} = 8000\ [\mathrm{J \cdot mol^{-1}}] \tag{26}$$

$$T_{transition} = 863.15\,\mathrm{K}\ . \tag{27}$$

The work of Seifert et al.[74] reports the value for the phase transition of K_3CrCl_6 as $\Delta H_{transition} = 7000\ [\mathrm{J \cdot mol^{-1}}]$. The choice of the value of the enthalpy of phase transition was made by considering the fact that Na_3CrCl_6 and K_3CrCl_6 have the same crystal structure. Figure 6 gives the calculated phase diagram for the system.

The comparison between the experimental and the calculated equilibrium points shows good agreement. The calculated eutectic point for $NaCl + Na_3CrCl_6$ (at $T = 873.49\,\mathrm{K}, x_{CrCl3} = 0.2107$) and $CrCl_3 + Na_3CrCl_6$ (at

---

[d] Studies on the structural properties of the NaCl-CrCl$_3$ salt system are scarce in the literature. Li et al.[72] performed X-ray and neutron scattering experiments as well as ab initio simulations. They have revealed the formation of $CrCl_6(3-)$ octahedral (around 65%) along with $CrCl_5(2-)$ species (around 20% to 30%) networks of $CrCl_6(3-)$ octahedral. However, it is not the scope of this paper to take the structural information into account for the thermodynamic modeling, as done recently on the LiF-UF$_4$ [73] or NaCl-UCl$_3$ [20] systems.

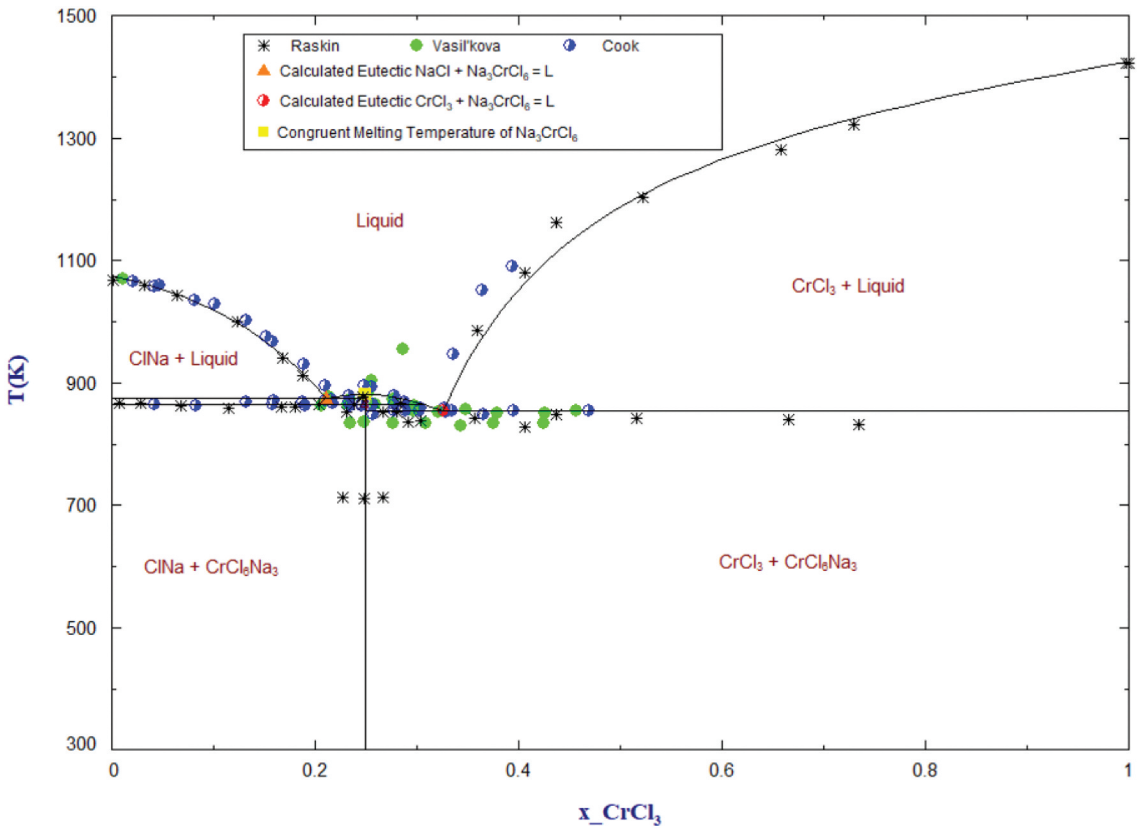

Fig. 6. Calculated phase diagram x_{CrCl_3} versus T[K] for NaCl-CrCl$_3$ system. Comparison with the experimental phase diagram data of Korshunov and Raskin,[15] Cook Jr.,[16] and Vasil'kova et al.[17]

$T = 853.11$ K, $x_{CrCl3} = 0.3254$) and the temperature for congruent melting of the intermediate solid at $T = 881.5$ K are in good agreement with the experimental values of Refs. [15], [16], and [17]. A detailed comparison is presented in Table XVI. However, similarly to the NaCl-CrCl$_2$ system, the NaCl-CrCl$_3$ system also requires more experimental thermodynamic data related to enthalpy of formation for the intermediate compound, the enthalpy of mixing of the liquid, activities, etc., to improve the developed thermodynamic model.

IV.C.3. FeCl$_2$-CrCl$_2$ System

For the FeCl$_2$-CrCl$_2$ system, the SNN coordination numbers for the liquid phase were set to the following values:

TABLE XVI

Comparison Between the Experimental and the Calculated Eutectic and Fusion Points for the NaCl-CrCl$_3$ System

Equilibrium Reaction	Calculated Value	Korshunov and Raskin[15]	Cook Jr.[16]	Vasil'kova et al.[17]
Eutectic $CrCl_3 + Na_3CrCl_6 = L$	$T = 853.11$ K $x_{CrCl_3} = 0.3254$	$T = 843$ K $x_{CrCl_3} = 0.314$	$T = 853$ K $x_{CrCl_3} = 0.34$	$T = 855$ K $x_{CrCl_3} = 0.31$
Congruent melting $Na_3CrCl_6 = L$	$T = 881.5$ K $x_{CrCl_3} = 0.25$	$T = 876$ K $x_{CrCl_3} = 0.25$	$T = 893$ K $x_{CrCl_3} = 0.25$	$T = 883$ K $x_{CrCl_3} = 0.25$
Eutectic $NaCl + Na_3CrCl_6 = L$	$T = 873.49$ K $x_{CrCl_3} = 0.2107$	$T = 866$ K $x_{CrCl_3} = 0.212$	$T = 870$ K $x_{CrCl_3} = 0.22$	$T = 866$ K $x_{CrCl_3} = 0.215$
Phase transition $Na_3CrCl_6(\alpha) = Na_3CrCl_6(\beta)$	$T = 863.15$ K —	$T = 713$ K —	$T = 863$ K —	$T = 835$ K —

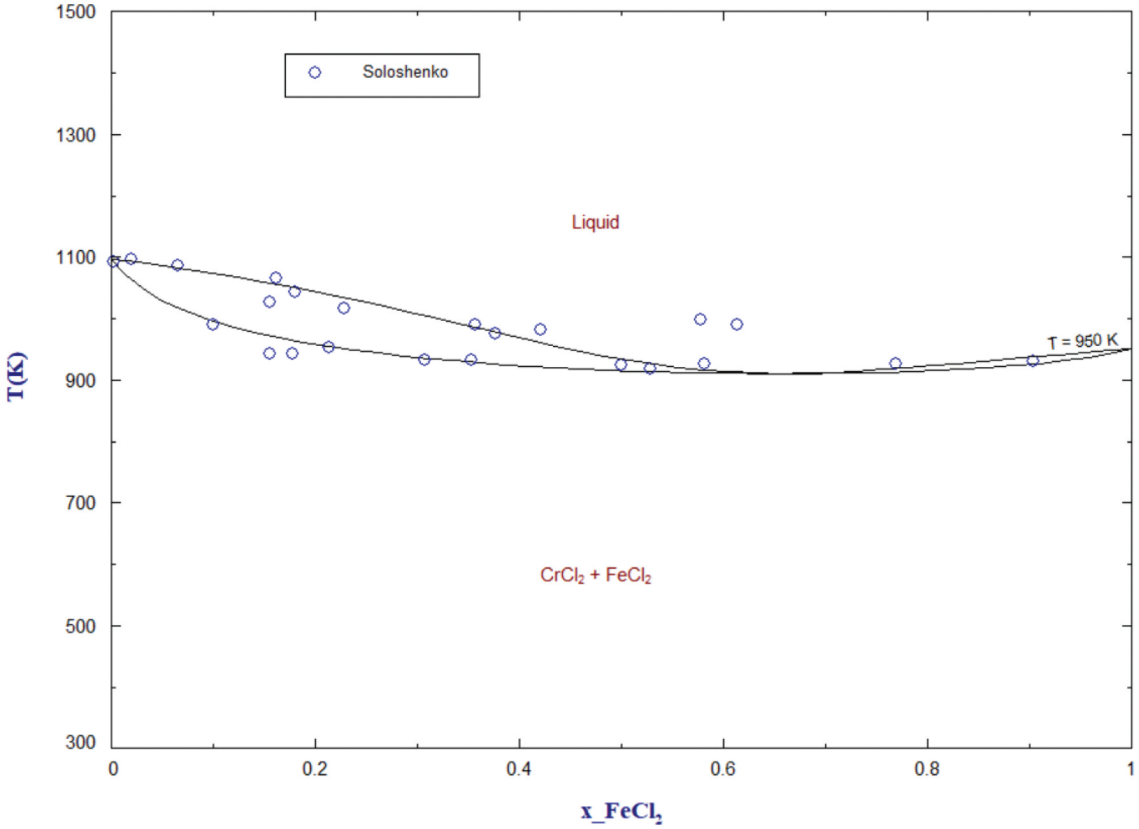

Fig. 7. Calculated phase diagram x_{FeCl_2} versus T[K] for FeCl$_2$-CrCl$_2$ system. Comparison with the experimental phase diagram data of Soloshenko and Vil'nyanskii.[18]

$$Z^{Fe}_{FeCr(II)} = Z^{Cr(II)}_{FeCr(II)} = 6 \quad (28)$$

$$Z^{Cl}_{FeCr(II)} = 3 \ . \quad (29)$$

The excess Gibbs energy associated with the quadruplet exchange reaction $\Delta g_{FeCr(II)/Cl}$ $[\mathrm{J \cdot mol^{-1}}]$ was optimized and expressed as

$$\Delta g_{FeCr(II)/Cl} = -4950\,[\mathrm{J \cdot mol^{-1}}] \ . \quad (30)$$

For the solid solution (Fe,Cr)Cl$_2$, the optimized excess Gibbs energy g^E $[\mathrm{J \cdot mol^{-1}}]$ is modeled as

$$g^E = 550 x_{FeCl_2} x_{CrCl_2}\,[\mathrm{J \cdot mol^{-1}}] \ , \quad (31)$$

where x_{FeCl_2} and x_{CrCl_2} represent the mole fraction of the pure end members. Figure 7 gives the calculated phase diagram for the system. The diagram shows good agreement with the liquidus curve points that have been estimated from the experimental phase diagram of Soloshenko and Vil'nyanskii.[18] However, thermodynamic data such as activities for the liquid and solid solutions would help improve the present model.

V. CONCLUSION

In the frame of the development of the JRCMSR database for MSRs, this paper presents the thermodynamic assessments of the pseudo-binary systems NaCl-CrCl$_2$, NaCl-CrCl$_3$, and FeCl$_2$-CrCl$_2$ to investigate the corrosion products forming due to interactions between the molten salt and the steel. Ab initio calculations have been performed to determine the missing thermodynamic properties of the two intermediate compounds Na$_2$CrCl$_4$ and Na$_3$CrCl$_6$. The Gibbs energy functions for the compounds and the liquid have been further optimized to reproduce the existing phase diagram data. MQMQA has been used to describe the liquid phase while the solid solution phases have been modeled using the Substitutional Solution model, wherever required. Good agreement is obtained with the available data on the three systems.

However, it should be noted that these systems lack experimental measurements to improve the description. Measurements of the enthalpy of formation for the intermediate compounds, the enthalpy of mixing, and activities in the liquid would be very useful. Following this work, other pseudo-binary systems containing $MgCl_2$, $FeCl_x$, $NiCl_x$ with $CrCl_2$ and $CrCl_3$ will be assessed.

Disclosure Statement

No potential conflict of interest was reported by the author(s).

Funding

A. L. Smith, J. A. Ocádiz Flores, and T. F. Abbink acknowledge funding from the MIMOSA project, grant number 101061142 funded by the European Union. Views and opinions expressed are however those of the author(s) only and do not necessarily reflect those of the European Union. Neither the European Union nor the granting authority can be held responsible for them.

ORCID

V. Tiwari http://orcid.org/0000-0002-9308-2855

References

1. H. LUKAS, S. FRIES, and B. SUNDMAN, *Computational Thermodynamics: The Calphad Method*, Cambridge University Press (2007).
2. C. ROBELIN, P. CHARTRAND, and A. D. PELTON, "Thermodynamic Evaluation and Optimization of the (NaCl+KCl+MgCl2+CaCl2+MnCl2+FeCl2+CoCl2 +NiCl2) System," *J. Chem. Therm.*, **36**, *9*, 809 (2004); https://doi.org/10.1016/j.jct.2004.05.005.
3. C. ROBELIN, P. CHARTRAND, and A. D. PELTON, "Thermodynamic Evaluation and Optimization of the (MgCl2+CaCl2+MnCl2+FeCl2+CoCl2+NiCl2) System," *J. Chem. Therm.*, **36**, *9*, 793 (2004); https://doi.org/10.1016/j.jct.2004.05.004.
4. J. ARD et al., "Thermodynamic Assessments or Reassessments of 30 Pseudo- Binary and -Ternary Salt Systems," *J. Chem. Therm.*, **177** (2022).
5. J. L. FLECHE, "Thermodynamical Functions for Crystals with Large Unit Cells Such as Zircon, Coffinite, Fluorapatite, and Iodoapatite from Ab Initio Calculations," *Phys. Rev. B*, **65**, 245116 (2002); https://doi.org/10.1103/PhysRevB.65.245116.
6. O. BENES, "Thermodynamics of Molten Salts for Nuclear Applications – JRC-ITU-TN- 2008/40," PhD Thesis, Institute of Chemical Technology, Prague, Faculty of Chemical Technology, Department of Inorganic Chemistry, Prague (2008).
7. H. SEIFERT and K. KLATYK, "Über die Systeme Alkalimetallchlorid/Chrom (II)-Chlorid," *Z. Anorg. Allg. Chem.*, **334**, *3–4*, 113 (1964); https://doi.org/10.1002/zaac.19643340302.
8. J. C. SHILOFF, "Thermal Analysis of the Chromous Chloride—Sodium Chloride System," *J. Phys. Chem.*, **64**, *10*, 1566 (1960); https://doi.org/10.1021/j100839a056.
9. B. KORSHUNOV, V. SAFONOV, and D. DROBOT, "Fusion Diagrams of Chloride Systems," *Reference Guide. "Khimiya"("Chemistry")* (1972).
10. A. EFIMOV, I. KOZHINA, and E. LUPENKO, "The Interaction in the Binary System NaCl-CrCl2," *Fiz. Khim*, **4**, 138 (1967).
11. S. SHKOL'NIKOV, *Tr. Leningrad Politekh. Inst*, **272**, 30 (1967).
12. P. VILLARS and K. CENZUAL, "Crystal Structure Database for Inorganic Compounds Tech. Rep. Pearson's Crystal Data" (2020).
13. R. KANNO et al., "Crystal Structure of Double Chlorides, Na_2MCl_4 (M=Mg, Cr, Cd): Correlation with Ionic Conductivity," *Solid State Ionics*, **39**, *3*, 233 (1990); https://doi.org/10.1016/0167-2738(90)90402-D.
14. T. OKI and J. TANIKAWA, "Equilibrium Phase Diagrams of $CrCl_3$-NaCl and $CrCl_3$-KCl Systems," *Electrochem. Ind. Phys. Chem.*, **36**, 119 (1968).
15. B. KORSHUNOV and B. RASKIN, "Interaction of Chromium (iii) Chloride with Sodium, Potassium, and Magnesium Chlorides in Molten State," *Zh. Neorganicheskoi Khimii*, **7**, *5*, 1137 (1962).
16. C. M. COOK JR., "The Systems NaCl $CrCl_3$ and KCl $CrCl_3$," *J. Inorg. Nucl. Chem.*, **25**, *1*, 123 (1963); https://doi.org/10.1016/0022-1902(63)80218-3.
17. I. VASIL'KOVA, A. EFIMOV, and B. PITIRIMOV, "Complex Formation in the MCl-$CrCl_3$ System (M = Alkali Metals)," *Zh. Neorganicheskoi Khimii*, **9**, 900 (1964).
18. A. SOLOSHENKO and Y. VIL'NYANSKII, "The FeCl2 - CrCl2 System," *Russian J. Inorganic Chem.*, **14**, *17*, 1045 (1969).
19. R. SHANNON, "Revised Effective Ionic Radii and Systematic Studies of Interatomic Distances in Halides and Chalcogenide," *Acta Crystallogr.*, **A32**, 751 (1976); https://doi.org/10.1107/S0567739476001551.
20. G. VAN OUDENAREN, J. OCADIZ-FLORES, and A. SMITH, "Coupled Structural-Thermodynamic Modelling of the Molten Salt System NaCl-UCl_3," *J. Molecular Liquids*, **342**, 117470 (2021); https://doi.org/10.1016/j.molliq.2021.117470.

21. V. GLUSHKO et al., *Thermodynamic Properties of Individual Materials* (1978) (in Russian).
22. R. DAWSON, E. BRAKETT, and T. BRAKETT, "A High Temperature Calorimeter; The Enthalpies of α-Aluminum Oxide and Sodium Chloride," *J. Phys. Chem.*, **67**, 1669 (1963); https://doi.org/10.1021/j100802a021.
23. I. MURGULESCU et al., "Heat Capacities in Molten Alkaline Halides," *Rev. Roumaine Chim.*, **22**, 683 (1977).
24. W. PLATO, "Erstarrung Erscheinungen an anorganischen Salzen und Salzgemischen. I," *Z. Phys. Chem.*, **55**, 721 (1906); https://doi.org/10.1515/zpch-1906-5542.
25. B. PYASHYENKO, *Metallurgiya*, **10**, 85 (1935).
26. H. VIITALA, P. TASKINEN, and D. LINDBERG, "Experimental Determination and Thermodynamic Optimization of the CuCl–$ZnCl_2$, $ZnCl_2$–$FeCl_3$, CuCl–$FeCl_3$, CuCl–$CuCl_2$, $FeCl_2$–$FeCl_3$, $FeCl_2$–$CuCl_2$ and CuCl–$PbCl_2$ Phase Equilibria," *Calphad*, **67**, 101667 (2019); https://doi.org/10.1016/j.calphad.2019.101667.
27. M. W. CHASE et al., *JANAF Thermochemical Tables* (1985).
28. R. GEE and R. SHELTON, "Thermodynamic Properties of $CrCl_3$ from Emf Measurements on Solid-Electrolyte Galvanic Cells Using the $CrCl_2$, $CrCl_3$ Electrode," *J. Less Common Metals*, **41**, 347 (1975); https://doi.org/10.1016/0022-5088(75)90041-7.
29. J. STOUT and R. CHISHOLM, "Heat Capacity and Entropy of $CuCl_2$ and $CrCl_2$ from 11 to 300 K. Magnetic Ordering in Linear Chain Crystals," *J. Chem. Phys.*, **36**, 979 (1962); https://doi.org/10.1063/1.1732699.
30. N. GREGORY and T. BURTON, "Heats of Formation of Chromium (III) and Chromium (II) Iodides," *J. Am. Chem. Soc.*, **75**, 6054 (1953); https://doi.org/10.1021/ja01119a517.
31. H. DOERNER, "Contributions to the Data on Theoretical Metallurgy," *US Department of the Interior, Bureau of Mines*, **577** (1937).
32. S. SCHUKAREV et al., "Thermodynamic Dissociation of Chromium Chloride and Bromide," *Russian J. Inorg. Chem.*, **1**, 1697 (1956).
33. K. JELLINEK and R. KOOP, "Über Heterogene Gleichgewichte von Metallhalogeniden Mit Wasserstoff Bzw. Chlorwasserstoff," *Z. Phys. Chem.*, **145**, 305 (1929); https://doi.org/10.1515/zpch-1929-14529.
34. D. D. WAGMAN, *Selected Values of Chemical Thermodynamic Properties*, Vol. 270, Institute for Materials Research, National Bureau of Standards (1965).
35. *Metallurgical Thermochemistry*, E. L. EVANS, C. ALCOCK, and O. KUBASCHEWSKI, Eds., Pergamon Press, Oxford (1967).
36. SGPS-SGTE. Pure Substances Database (v13.1), Accessed via FactSage (Version 7.2), Scientific Group Thermodata Europe: Saint-Martin-d'Hères.
37. V. IORISH et al., *The IVTAN Data Bank on the Thermodynamic Properties of Individual Substances* (1978).
38. H. DOERNER, "Chemistry of the Anhydrous Chlorides of Chromium: A Thermodynamic Investigation," U.S. Department of the Interior, Bureau of Mines (1937).
39. K. SANO, *J. Chem. Soc. Japan*, **59**, 937 (1938).
40. K. SANO, *Chem. Abstr*, **32**, 8246 (1938).
41. E. MANNEI, E. ASEDEGBEGA-NIETO, and F. AYARI, "Thermal Treatment of Anhydrous Chromium (III) Chloride: Thermodynamic Study," *Thermochim. Acta*, **707**, 179102 (2022); https://doi.org/10.1016/j.tca.2021.179102.
42. D. Wagman, "The NBS tables of chemical thermodynamic properties. Selected values for inorganic and C1 and C2 organic substances in SI units." *Tech. rep. National Standard Reference Data System* (1982).
43. I. BARIN, O. KNACKE, and O. KUBASCHEWSKI, *Thermochemical Properties of Inorganic Substances: Supplement*, Springer Science and Business Media (2013).
44. C. T. ANDERSON, "The Heat Capacities of Chromium, Chromic Oxide, Chromous Chloride and Chromic Chloride at Low Temperatures," *J. Am. Chem. Soc.*, **59**, 488 (1937); https://doi.org/10.1021/ja01282a019.
45. G. MOORE, "Heat Contents at High Temperatures of the Anhydrous Chlorides of Calcium, Iron, Magnesium and Manganese," *J. Am. Chem. Soc.*, **65**, *9*, 1700 (1943); https://doi.org/10.1021/ja01249a014.
46. R. MATSUZAKI, H. MORITA, and Y. SAEKI, "Properties of Chromium Trichloride," *J. Chem. Soc. Japan. Industr. Chem. Sec.*, **74**, 1592 (1971).
47. S. SCHUKAREV et al., "Enthalpy of Formation for Chromium Trichloride," *Russian J. Inorg. Chem.*, **11**, 247 (1966).
48. B. TIMOFEYEV and V. YULDASHEVA, "Enthalpy of Formation of Chromium (III) Chloride," *J. Chem. Thermodynamics*, **22**, 417 (1990); https://doi.org/10.1016/0021-9614(90)90131-9.
49. W. HANSEN and M. GRIFFEL, "Heat Capacities of CrF_3 and $CrCl_3$ from 15 to 300 K," *J. Chem. Phys.*, **28**, 902 (1958); https://doi.org/10.1063/1.1744294.
50. L. ZELENINA et al., "Tensimetric Investigation of the $CrCl_3$-Cl_2 System in the Temperature Range of 600–1200 K," *Russ. Chem. Bull. Int. Ed.*, **53**, 1621 (2004); https://doi.org/10.1007/s11172-005-0006-0.
51. M. KOSTRYUKOVA, "Heat Capacity of Anhydrous Chlorides of the Iron Group at Low Temperatures," *J. Exp. Theory Fiz.*, **55**, *2*, 453 (1968).
52. M. KOSTRYUKOVA and L. LUKYANOVA, "Heat Capacity of Anhydrous $CrCl_3$ at Low Temperatures," *J. Exp. Theory Fiz.*, **61**, *2*, 732 (1971).

53. D. KERRIDGE and I. STURTON, “Fused Zinc Chloride Part II: Some Solubility Measurements,” *Inorgan. Chim. Acta*, **8**, 27 (1974); https://doi.org/10.1016/S0020-1693(00)92591-X.
54. I. VASIL’KOVA, A. EFFIMOV, and B. PITIRIMOV, “Enthalpy of Formation of Na3CrCl6, K3CrCl6, and K3Cr2Cl9,” *Zh. Neorganicheskoi Khimii*, **9**, 754 (1964).
55. S. SCHUKAREV et al., “Enthalpies of Formation of the Alkali Metal Chlorochromates (III),” *Russian J. Inorg. Chem.*, **11**, 268 (1966).
56. S. J. CLARK et al., “First Principles Methods Using CASTEP,” *Z. Kristallogr. Crystalline Mater.*, **220**, *5–6*, 567 (2005); https://doi.org/10.1524/zkri.220.5.567.65075.
57. J. P. PERDEW et al., “Restoring the Density-Gradient Expansion for Exchange in Solids and Surfaces,” *Phys. Rev. Lett.*, **100**, 136406 (2008); https://doi.org/10.1103/PhysRevLett.100.136406.
58. J. D. PACK and H. J. MONKHORST, “Special Points for Brillouin-Zone Integrations—A Reply,” *Phys. Rev. B*, **16**, 1748 (1977); https://doi.org/10.1103/PhysRevB.16.1748.
59. P. VILLARS and K. CENZUAL, *Pearson’s Crystal Data—Crystal Structure Database for Inorganic Compounds*, ASM International (2011).
60. P. VINET et al., “Temperature Effects on the Universal Equation of State of Solids,” *Phys. Rev. B*, **35**, 1945 (1987); https://doi.org/10.1103/PhysRevB.35.1945.
61. P. PERROT, *Propriétés thermodynamiques des composés minéraux: Partie 3*, Techniques de l’Ingénieur.
62. C. GUÉNEAU, M. ASTA, and B. SUNDMAN, “1.26 – Computational Thermodynamics: Application to Nuclear Materials,” *Comprehensive Nuclear Materials*, 2nd ed., Vol. 1, p. 814, R. J. KONINGS and R. E. STOLLER, Eds., Elsevier.
63. A. D. PELTON, P. CHARTRAND, and G. ERIKSSON, “The Modified Quasi-Chemical Model: Part IV. Two-Sublattice Quadruplet Approximation,” *Metall. Mater. Trans. A*, **32**, *6*, 1409 (2001); https://doi.org/10.1007/s11661-001-0230-7.
64. P. CHARTRAND and A. D. PELTON, “Thermodynamic Evaluation and Optimization of the Li, Na, K, Mg, Ca//F, Cl Reciprocal System Using the Modified Quasi-Chemical Model,” *Metall. Mater. Trans. A*, **32**, *6*, 1417 (2001); https://doi.org/10.1007/s11661-001-0231-6.
65. A. D. PELTON et al., “The Modified Quasichemical Model I—Binary Solutions,” *Metall. Mater. Trans. B*, **31**, *4*, 651 (2000); https://doi.org/10.1007/s11663-000-0103-2.
66. A. D. PELTON and P. CHARTRAND, “The Modified Quasi-Chemical Model: Part II. Multicomponent Solutions,” *Metall. Mater. Trans. A*, **32**, *6*, 1355 (2001); https://doi.org/10.1007/s11661-001-0226-3.
67. A. D. PELTON and P. CHARTRAND, “Thermodynamic Evaluation and Optimization of the LiCl-NaCl-KCl-RbCl-CsCl-MgCl$_2$-CaCl$_2$ System Using the Modified Quasi-Chemical Model,” *Metall. Mater. Trans. A*, **32**, *6*, 1361 (2001); https://doi.org/10.1007/s11661-001-0227-2.
68. P. CHARTRAND and A. D. PELTON, “Thermodynamic Evaluation and Optimization of the LiF-NaF-KF-MgF$_2$-CaF$_2$ System Using the Modified Quasi-Chemical Model,” *Metall. Mater. Trans. A*, **32**, *6*, 1385 (2001); https://doi.org/10.1007/s11661-001-0228-1.
69. A. SMITH et al., “A New Approach for Coupled Modelling of the Structural and Thermo-Physical Properties of Molten Salts. Case of A Polymeric Liquid LiF-BeF$_2$,” *J. Molecular Liquids*, **299**, 112165 (2020); https://doi.org/10.1016/j.molliq.2019.112165.
70. T. M. BESMANN and J. SCHORNE-PINTO, “Developing Practical Models of Complex Salts for Molten Salt Reactors,” *Thermo*, **1**, *2*, 168 (2021); https://doi.org/10.3390/thermo1020012.
71. C. GUÉNEAU et al., “Thermodynamic Modeling of the Uraniumn-Tellurium System: Estimation of the Uncertainties by a Bayesian Approach,” *Thermo*, **2**, *1*, 15 (2022); https://doi.org/10.3390/thermo2010003.
72. Q. LI et al., “Complex Structure of Molten NaCl–CrCl$_3$ Salt: Cr–Cl Octahedral Network and Intermediate-Range Order,” *ACS Appl. Energy Mater.*, **4**, *4*, 3044 (2021); https://doi.org/10.1021/acsaem.0c02678.
73. J. OCÁDIZ-FLORES et al., “New Insights and Coupled Modelling of the Structural and Thermodynamic Properties of the LiF-UF$_4$ System,” *J. Molecular Liquids*, **331**, 115820 (2021); https://doi.org/10.1016/j.molliq.2021.115820.
74. H. F. J. FRIEDRICH et al., “Uber Alkali-hexachlorochrornate(III): Na3CrCl6,” *Z. Anorg. Allg. Chem.*, **548**, 141 (1987); https://doi.org/10.1002/zaac.19875480516.